Xe-100 Licensing Topical Report
Reactor Core Design Methods and Analysis

Document ID Number	**:**	**006889**
Configuration Classification	**:**	**XE00-GL-GL-GL-GL-GL-X**
Revision	**:**	**1**
Security Classification	**:**	**Non Proprietary**
Status	**:**	**Approved**
Date Created	**:**	**04-Apr-2024**
Project	**:**	**XE-100**

E-SIGNATURES

Document Approval Signees

Action	Designation	Name	Signature	Date
Preparer	Principal Consultant	Jose Garcia	Maintained in Teamcenter	April 5, 2024
Reviewer	Lead, Nuclear Engineering	Sonat Sen	Maintained in Teamcenter	April 5, 2024
Reviewer	Lead, Component Thermal Hydraulics	Wian Van Der Merwe	Maintained in Teamcenter	April 5, 2024
Reviewer	Engineer VI, Licensing	Mark Paul	Maintained in Teamcenter	April 5, 2024
Reviewer	Senior Vice President, Chief Scientist	Eben Mulder	Maintained in Teamcenter	April 6, 2024
Approver	Director, Licensing	Stephen Vaughn	Maintained in Teamcenter	April 7, 2024

10 CFR 810 EXPORT-CONTROLLED INFORMATION DISCLAIMER

This document was reviewed by X-energy and determined to not contain information designated as export-controlled per Title 10 of the Code of Federal Regulations (CFR) Part 810 or 10 CFR 110.

DEPARTMENT OF ENERGY ACKNOWLEDGEMENT AND DISCLAIMER

This material is based upon work supported by the Department of Energy under Award Number DENE0009040.

SYNOPSIS

This Licensing Topical Report (LTR) describes X Energy, LLC's (X-energy) methods and computer codes used to support the Xe-100 reactor core physics analysis. The Xe-100 is a 200 MWt (80 MWe) pebble bed high-temperature gas-cooled reactor design.

The development of the core physics methods and codes is in accordance with the regulatory requirements discussed in Section 1. This report provides the overall framework and approach to develop specific code methodologies and their Verification and Validation (V&V). As documented throughout the report, validation and verification activities will be completed as planned and will be provided to the NRC staff through a revision to this report and continued engagements as needed.

The two physics computer codes described in this report are VSOP [4] and Siemens Simcenter STAR-CCM+ [5]. VSOP [4] is a computer code system for the comprehensive numerical simulation of the physics of thermal reactors and used extensively in modeling of pebble bed type gas-cooled reactors. STAR-CCM+ [5] is a Computational Fluid Dynamics (CFD) code, which will be used primarily to provide pebble flow characteristics in the Xe-100 pebble bed core.

The information from this LTR can be used to support safety analysis reports for prospective Xe-100 licensing applications under 10 CFR 50, 10 CFR 52, and/or 10 CFR 53.

The development and use of the reactor core design methods and analysis described in this report are subject to the applicable requirements of the NRC-approved X-energy Topical Report XEQAPD 1.0, "Quality Assurance Program Description" [26]. Accordingly, software used to produce analysis results that cannot, or will not, be independently verified by checking during the analysis (i.e., verifying, such as with the typical use of Excel or Mathcad, that the inputs entered each applicable set of equations produce the resulting outputs) shall be approved for use by issuing a Software Certificate. Qualified Software may be acquired, developed by X-energy, or commercial grade dedicated for use as described in the X-energy Quality Assurance procedure, "Software Procedure" [27]. X-energy plans on using the commercial grade dedication process for VSOP [4] while STAR CCM+ [5] is developed under an acceptable quality assurance program.

CONFIGURATION CONTROL/DOCUMENT CHANGE HISTORY

Document Change History

Rev.	Date	Preparer	Page/Section Revised	Description
1	04-Apr-2024	Jose Garcia	Complete	Initial issue

Table of Contents

List of Tables

List of Figures

Abbreviations/Acronyms

Short Form	Phrase
ABS	Acrylonitrile Butadiene Styrene
AGR	Advanced Gas Reactor
ANL	Argonne National Laboratory
AVR	Arbeit Gemeinschaft Versuchsreaktor Reactor
CFD	Computational Fluid Dynamics
CFR	Code of Federal Regulations
DEM	Discrete Element Method
EM	Evaluation Model
FE	Fuel Elements (Fuel Pebbles)
GE	Graphite Elements
GT-MHR	Gas Turbine Modular Helium Reactor
HTGR	High Temperature Gas-Cooled Reactor
HTR	High Temperature Reactor
IAEA	International Atomic Energy Agency
INET	Institute of Nuclear and New Energy Technology, Tsinghua University, Beijing, China
IPyC	Inner Pyrolytic Carbon
KAERI	Korean Atomic Energy Research Institute, Daejeon, South Korea
LEU	Low Enriched Uranium
MCNP	Monte Carlo NParticle
MWe	Megawatt Electric
MWt	Megawatt Thermal
NEA	Nuclear Energy Agency
NGNP	Next Generation Nuclear Plant
NQA-1	Nuclear Quality Assurance
NRC	U.S. Nuclear Regulatory Commission
OPyC	Outer Pyrolytic Carbon
ORNL	Oak Ridge National Laboratory
PBMM	Pebble Bed Micro Model
PBMR	Pebble Bed Modular Reactor
PDC	Principle Design Criteria
PVC	Poly-Vinyl Chloride

Abbreviations/Acronyms

Short Form	Phrase
RCS	Reactivity Control System
RSS	Reactivity Shutdown System
RG	Regulatory Guide
RPV	Reactor Pressure Vessel
SiC	Silicon Carbide
TRISO	TRIstructural ISOtropic
UCO	Uranium Oxycarbide
VHTR	Very High Temperature Reactor
VSOP	Very Superior Old Programs
X-energy	X Energy, LLC

Definitions

Phrase	Definition
Commercial Grade Dedication	An acceptance process performed in accordance with NQA-1 to provide reasonable assurance that a commercial grade item or service will perform its intended safety function and, in this respect, is deemed equivalent to an item or service designed and manufactured or provided under the requirements of NQA-1. [23]
Verification	The process of determining whether or not the products of a given phase of the computer program development cycle fulfil the requirements established during the previous phase.
Validation	A process to assess fitness and quantify computer program accuracy for its intended applications by comparison of key physical parameters calculated in the computer code against relevant measured data or known analytical or numerical solutions.

1. Introduction

X Energy, LLC (X-energy) is developing the helium-cooled Xe-100 modular High-Temperature Gas-Cooled Reactor (HTGR) as an innovative nuclear energy solution. This reactor utilizes U.S.-developed Uranium Oxy-Carbide (UCO) TRISO [1] fuel which is encapsulated in spherical fuel elements known as fuel pebbles. The Xe-100 is designed to generate steam for traditional electricity purposes and also for various non-traditional applications of nuclear energy, such as supplying secure government installations, serving small or isolated grids, and providing steam for industrial processes.

1.1 Purpose

This report describes the reactor core design analysis methodology and computer codes used to analyze the Xe-100 reactor at the beginning of life, startup, power ascension, and at equilibrium conditions. This methodology is tailored for the development and assessment of the core design for normal operation and subsequent utilization in nuclear safety assessments specific to the Xe-100.

The primary objective of this report is to establish the reactor core design methods and the ability of the VSOP [4] and STAR-CCM+ [5] codes to accurately simulate the behavior of the Xe-100 reactor. The verification and validation process, as detailed in plans [8] [9], ensures the suitability of these codes as tools for modeling reactor core behavior.

1.2 Scope and Document Layout

Section 2 of this document provides an overview of the Xe-100 reactor design, including specifics of the TRISO-coated particle fuel and the pebble fuel design. Section 3 provides a summary of the physics models employed in the code, while Section 4 presents typical results for the Xe-100 reactor that support safety analyses. The sub-sections of Sections 5 and 6 outline the plans for validation and verification of the code. Section 7 briefly examines the alignment of the activities outlined in this report with the requirements of the NRC-approved X-energy Quality Assurance Program. Section 8 provides conclusions and limitations.

1.3 Interfacing Documents

This Licensing Topical Report (LTR) is one of several reports covering key regulatory issues submitted to the US Nuclear Regulatory Commission (NRC) staff as part of Xe-100 pre-application process. The X-energy reactor core design and analysis methodology is part of the overall approach to implement a risk-informed, performance-based design and licensing basis as described in Nuclear Energy Institute (NEI) 18-04 [28] and endorsed and clarified by NRC Regulatory Guide (RG) 1.233, [29]. This LTR interfaces with the follow documents:

- Xe-100 Licensing Topical Report, “Principal Design Criteria”. [2].
- Xe-100 Licensing Topical Report, “TRISO-X Pebble Fuel Qualification Methodology” [6], provides the technical foundation for the fuel qualification approach as well as the planned fuel

fabrication, irradiation, safety testing activities, and approach to qualify the Xe-100 fuel (UCO TRISO-coated particles).

- Xe-100 Licensing Topical Report, "GOTHIC and Flownex Analysis Codes Qualification" [34] presents the acceptability of these codes to model the LBEs in support of the X-energy safety analysis.
- Xe-100 Licensing Topical Report, "Transient and Safety Analysis Methodologies" [30], describes the methods and models used to determine offsite dose and control room dose resulting from licensing basis events (LBEs) identified in the PRA and related safety analyses.
- Xe-100 Licensing Topical Report, "Mechanistic Source Term Approach" describes the methodology employed to determine the source term for the X-100 reactor [31].

1.4 Regulatory Requirements and Guidance

The nuclear methodologies described herein support compliance with regulatory requirements and provide inputs to the Xe-100 safety analyses.

1.4.1 Regulatory Requirements

The Xe-100 reactor core design methods and analyses provide input to the Xe-100 safety analyses required to comply with the appropriate portions of:

- 10 CFR 50.34(a) (Construction Permits)
- 10 CFR 50.34(b) (Operating Licenses)
- 10 CFR 52.17(a)(1)(ix) (Early Site Permits)
- 10 CFR 52.47(a)(2)(iv) (Design Certifications)
- 10 CFR 52.79(a)(1)(vi) (Combined Licenses)
- 10 CFR 52.137(a)(2)(iv) (Design Approvals)
- 10 CFR 52.157(d) (Manufacturing Licenses)
- 10 CFR 100 (Reactor Site Criteria)

1.4.2 Regulatory Guidance

1.4.2.1 Policy Statement on the Regulation of Advanced Reactors

The Advanced Reactor Policy Statement [22] provides overarching guidance to advanced reactor developers like X-energy and informs the approach addressing regulatory requirements. The final policy statement includes multiple design attributes that could assist the NRC to establish the acceptability and/or ability to license advanced reactor designs. These attributes inform the way X-energy assessed the 10 CFR Part 50 technical requirements associated with design and programmatic elements of the Xe-100.

1.4.2.2 RG 1.231, Acceptance of Commercial-Grade Design and Analysis Computer Programs Used in Safety-Related Applications for Nuclear Power Plants

Regulation Guide 1.231 [25] provides guidance to licensees when the licensees choose to use evaluation models that have not been developed under American Society of Mechanical Engineers (ASME) NQA-1-2015, “Quality Assurance Program Requirements for Nuclear Facilities,” [23]. Under this Reg Guide the NRC endorses EPRI Technical Report 1025243 Rev 1, Plant Engineering: Guideline for the Acceptance of Commercial-Grade Design and Analysis Computer Programs Used in Safety-Related Applications [24]. This EPRI report provides an acceptable process to take a commercially available Evaluation Model (EM) and make it acceptable for use in safety-related applications.

1.5 Outcome Objectives

X-energy is requesting NRC review and approval of the methodology and computer codes described in Sections 3, 4, 5, and 6 of this LTR for use in Xe-100 license applications as an appropriate means to perform steady-state and normal operations physics analysis and to provide appropriate inputs to support the Xe-100 safety analyses.

2. Xe-100 Design Overview

The Xe-100 reactor, with a thermal output of 200 MW, generates high-grade, super-heated steam at 565°C and 16.5 MPa pressure. It is suitable for various energy applications, including electricity generation, industrial process heating, district heating, desalination, and augmenting wind/solar power, either independently or in combination [3].

2.1 Xe-100 Reactor Design

The general concept of HTGRs has progressed from earlier designs utilizing air or carbon dioxide for cooling. The adoption of helium as the heat transfer medium and graphite as the moderator has led to improved neutronic and thermal efficiencies, as well as advanced safety features. Internationally, two reactor core configurations, namely the pebble bed core and a prismatic core, have been developed for commercial modular HTGR designs [6].

The Xe-100 reactor design is based on a pebble bed core configuration. Pebble bed reactor technology dates back to the late 1960s, when the 46 MWt Arbeitsgemeinschaft Versuchsreaktor (AVR) was designed and operated in Germany. Later, advanced pebble bed reactor designs were developed in Germany, South Africa, and China. The Chinese have a modular HTGR pebble bed reactor design, the HTR-PM, with two 250 MWt reactor modules serving a single 200 MWe turbine/generator, that entered commercial operation as of December 2023 [7]. The Xe-100 reactor and steam generator systems are shown in Figure 1.

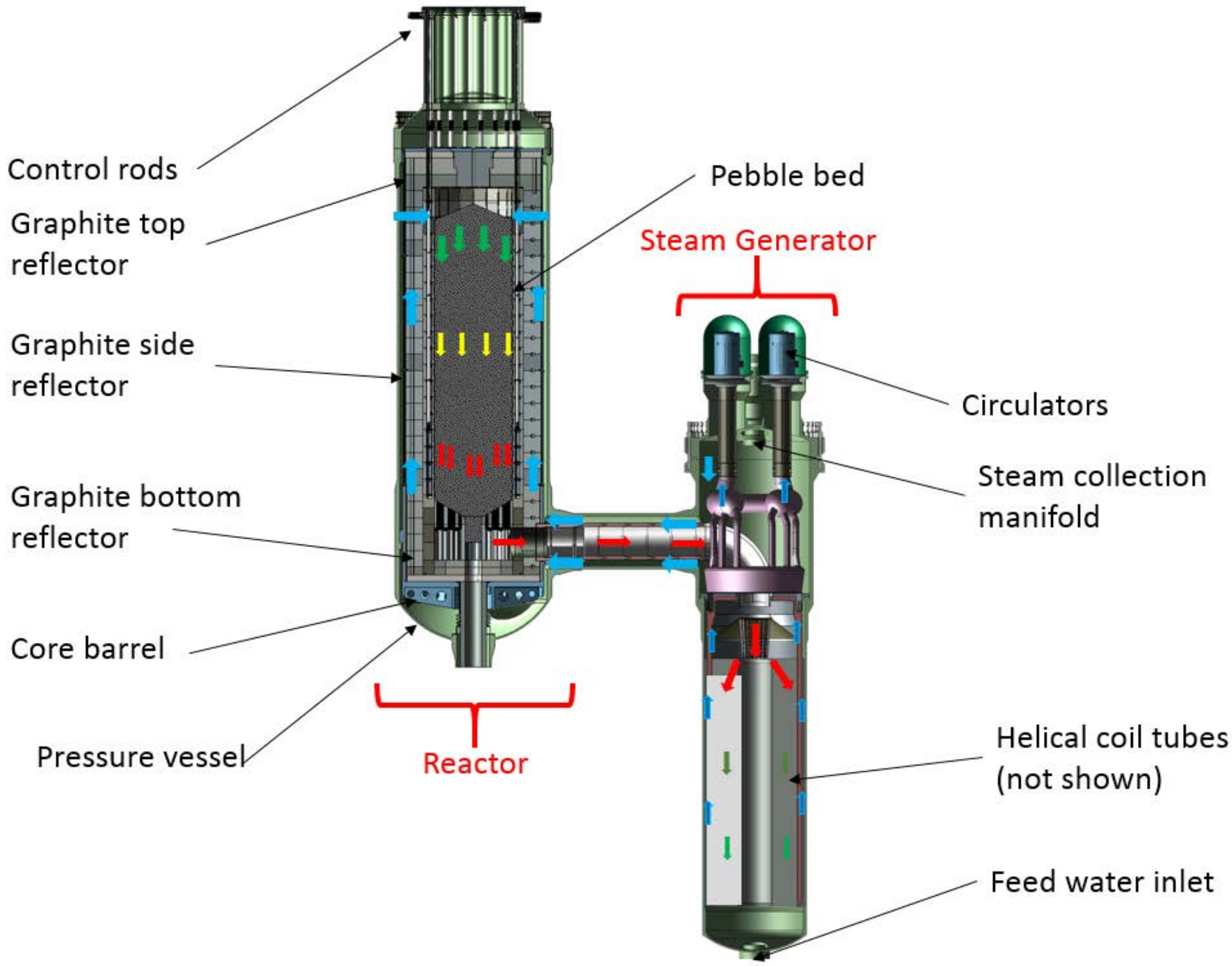

Figure 1: Xe-100 Section View

2.2 Reactor Core Design

The reactor core consists of a cylindrical pebble bed region, the upper and lower conic regions, the fueling region, the defueling chute, coolant inlet and outlet channels in the reflector, engineered channels in the reflector, and the reactivity control and shutdown system. The main reactor core characteristics, including dimensions, thermal power, and major operating conditions are given in Table 1 [6] [35].

The core is the region of the pebble bed that produces considerable fission power density, determined as the region from the top of the upper conic region of the core to the bottom of the lower conic region of the core. A representative pebble core layout is presented in Figure 2. Core geometrical characteristics such as the conic regions and defueling chute are designed to support a more uniform burnup and fuel performance in the core, as the conic regions and relative diameters of the fueling chute and cylindrical section impact pebble velocity profile and residence time. The fueling region, situated at the core's top, guide pebbles from the insertion line into the core, while the defueling chute, located at the bottom, serves as a subcritical region allowing for adequate decay of short-lived fission products before pebbles enter the region for testing the pebble physical integrity, followed by the gamma-spectrometric burnup measurement area.

Coolant inlet and outlet channels within the reflector, designed for reduced pressure losses and optimal flow distribution through the pebble bed core, are positioned in the top- and bottom reflectors, respectively. The block-type reflector design includes radial and axial spoke gaps, minimizing helium bypassing the core region. Engineered channels within the graphite blocks facilitate the movement of ex-core reactivity control elements.

The active core volume accommodates approximately 224,000 spherical fuel elements, referred to as pebbles, forming the pebble bed. Each pebble comprises roughly 19,000 TRISO-coated particles pressed into a hardened matrix graphite sphere of 6 cm diameter. Pebbles are introduced into the core during reactor operation via a central tube at the top of the reactor pressure vessel (RPV). A fuel discharge system at the bottom of the core expels pebbles through the RPV's lower section to the Burn-up Measurement System for individual assessment regarding physical integrity and burn-up levels.

Based on their burnup, the pebbles may be directed to the spent fuel storage or returned to the top of the RPV, where they are reinserted into the core. Typically, a pebble goes through this process six times before reaching burn-up limits and being removed from reactor operation. Spent fuel pebbles are inventoried and stored in spent fuel casks for storage.

The core excess reactivity is limited by online refueling because the fuel can be loaded and unloaded as desired during full power operation. The Xe-100 has an overall negative temperature coefficient of reactivity due to the Doppler broadening of the fuel kernel content and the moderator temperature coefficient, which ensures a negative reactivity insertion during licensing basis events that increase fuel temperatures. This inherent reactivity feedback characteristic is one of the primary safety features the fuel provides during transient and safety analyses calculations and allows the Xe-100 to achieve a safe shutdown condition.

Table 1: Xe-100 Reactor Main Characteristics

Thermal power	200 MWt	Helium flow rate (excluding bypass)	[[ ]]^{P}
Core volume	[[ ]]^{P}	Helium pressure	6 MPa
Core average power density	[[ ]]^{P}	Pebble packing fraction	[[ ]]^{P}
Height (flattened pebble bed)	[[ ]]^{P}	Particle packing fraction	[[ ]]^{P}
Diameter of pebble bed	[[ ]]^{P}	Burnup	163 GWd/MTU
Average pebble passes through the core	6	Enrichment	15.5%
Heavy metal loading per pebble	[[ ]]^{P}	Moderation ratio (C/U)	[[ ]]^{P}
TRISO-coated particles per pebble	~19,000	U-235 per pebble	[[ ]]^{P}
Gas inlet temperature	[[ ]]^{P}	Daily pebble charge	[[ ]]^{P}
Gas outlet temperature	750°C	Average fuel residence time	[[ ]]^{P}

^{P} Refers to proprietary information

[[

]]P

Figure 2: Representative X-100 Pebble Core Configuration

2.3 Fuel Pebble Design

The defining characteristic of the pebble bed reactor and the key to the safety and operational simplicity of the Xe-100 is the use of TRISO-coated fuel particles embedded in fuel pebbles. The design of the coated particles and fuel pebbles, including their nominal dimensions, is depicted in Figure 3.

Figure 3: Xe-100 Reference Fuel Element (Fuel Pebble) Design

As shown in Figure 3, the 60 mm-diameter spherical fuel pebble consists of two zones: the inner spherical region is known as the fuel core zone, and the outer shell surrounding the fuel region is known as the fuel free zone. The 50-mm diameter fuel zone of each fuel pebble contains approximately 19,000 thousand TRISO-coated fuel particles evenly distributed in a carbonaceous matrix material. The fuel-free zone is a 5 mm thick shell of the same matrix material formed by a high-pressure isostatic pressing process and machined to final dimensions. X-energy has selected the U.S. equivalent of the German A3-3 ("US A3-3") matrix as the reference matrix for the Xe-100 fuel element, also referred to as a fuel pebble. The relatively low particle packing fraction in the fuel zone [[ ]]^{P} and pebbles being fully wetted by the helium everywhere, lead to low-temperature gradients across the fuel particle and lower maximum fuel temperatures during normal operation.

2.4 TRISO-Coated Particle Fuel

Coated particle fuel has been used in HTGRs since their inception in the early 1960s. TRISO-coated particle fuel was first introduced in the Dragon reactor, and Fort St. Vrain (FSV) was the first electricity producing HTGR with an all TRISO-coated particle core. TRISO-coated particle fuel has been the fuel of choice for all modular HTGR designs, beginning with the German pebble bed HTR-Modular and the Modular High-Temperature Gas-Cooled Reactor program in the U.S.

In the Xe-100 design, the TRISO fuel particles consist of a Uranium Oxycarbide (UCO) fuel microsphere ("kernel"), 425 µm in diameter and coated with multiple layers of pyrolytic carbon and silicon carbide (SiC) as shown in Figure 4. UCO was chosen for the Xe-100 design to take advantage of the ongoing advanced gas reactor (AGR) Fuel Development and Qualification Program at Idaho National Laboratory and Oak Ridge National Laboratory. The AGR Program is focused on qualifying UCO TRISO fuel and is being conducted under a quality assurance program that meets Nuclear Quality Assurance (NQA-1) [23] requirements and has been reviewed and found by the NRC staff to be acceptable for use during the technology development phase of the NGNP Project; results to date have been excellent. The performance of TRISO-coated particles made to AGR 1/2 specifications (identical coating structure, but different kernel and particle size, enrichment, and burn-up) was provided to the NRC staff for formal review in 2019 and received a favorable safety evaluation [1] in August 2020.

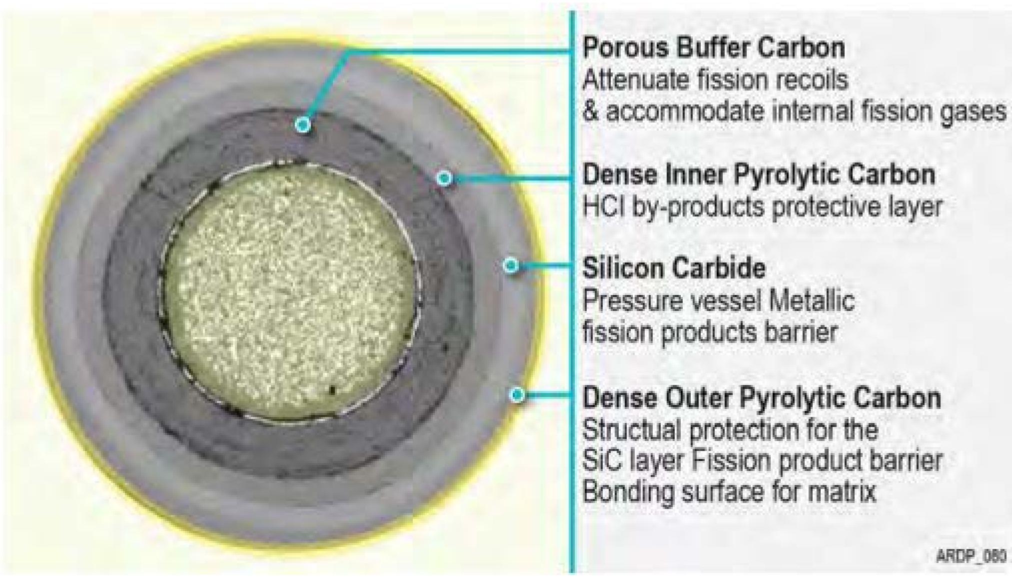

Figure 4: TRISO Fuel Particle Configuration and Coating Functions

While the Xe-100 design has evaluated several fuel specifications that could be used safely in operation, the reference Xe-100 fuel particle chosen is the same as the 15.5%-enriched, 425-µm UCO TRISO-coated particles irradiated in the AGR-5/6/7 qualification/margin test. The finished particle nominal diameter is 855 µm. The different coating layers, consisting of the buffer, inner pyrolytic carbon (IPyC), SiC, and outer pyrolytic carbon (OPyC) layers are referred to collectively as a TRISO coating. The coating system constitutes a miniature multi-shell pressure vessel that provides retention of the fission products that are generated by the fissioning of the nuclear material in the kernel. A substantial fraction of the fission products is retained inside the kernel itself. The performance of these coatings directly supports the functional containment approach for evaluating the Xe-100 design in transient and safety analyses.

The four coating layers of a TRISO-coated particle have specialized purposes as shown in Figure 4, but in composite, they constitute a high-integrity pressure vessel that retains fission products. The physical properties and performance capabilities of the TRISO-coated particles are among the most important factors impacting the radiological safety of the HTGR. This is because fission product retention in the fuel, as well as the high fuel burnups and temperatures that can be tolerated in the reactor core, are primarily determined by the fuel particle properties.

2.5 Control and Shutdown Rods

Although the negative temperature coefficient provides the primary reactivity control, its response is slightly delayed as heat-up first needs to occur before the reactivity is reduced. This delayed reaction would result in the reactor temperature increasing and hence the steam temperature would also increase. To control the overshoot to remain within limits typically required for a steam turbine, an active control bank is used to trim the reactor temperature and hence control the steam temperature to within the operational band needed for the steam turbine. The control bank is comprised of [[ ]]^{P} control rods. The control rods are inserted into cylindrical channels in the side reflector positioned close to the pebble bed core. The control rods are made up of [[ ]]^{P}. The control rods are manufactured from Incoloy 800H with an annular zone of boron carbide B_4C sandwiched between an inner and outer Incoloy cylinder.

The shutdown bank, also comprised of [[ ]]^{P} rods, are identical to the control rods in both design and manufacture but are not used to control reactivity at power. Shutdown bank is either fully inserted or fully withdrawn and will automatically insert when power is removed from their control drive mechanisms assisted by the force of gravity.

2.6 Core Reflector

The core graphite assembly provide the reactor with the core geometry which forms a cylindrical volume that contains the fuel pebbles. The core graphite assembly consist of [[ ]]^{P} The graphite blocks primarily provide:

- Core geometry
- Neutron reflection and some moderation
- Definition for the core coolant flow path
- Online fueling - and defueling routes for the fuel
- Shielding
- Thermal insulation for metallic structures
- Channels for the insertion of control and shutdown rods

3. Overview of Core Physics

3.1 Core Modeling

The Xe-100 core configuration is double-heterogeneous and non-stationary. The pebble bed continuously evolves from an early startup phase to a statistically steady burnup equilibrium condition. The Xe-100 core physical characteristics such as core geometry, double-heterogeneity, and pebble bed motion require unique modeling approaches.

The core physics methodology and codes developed for core design and analysis align closely with the physical behavior of the core. The Xe-100 core model includes neutronic and thermal-hydraulics modules with several degrees of explicit coupling between them.

The neutronic analyses of the Xe-100 core accounts for the double-heterogeneity of TRISO particles and pebbles without any need of performing validation of lower order methods. The explicit neutronic model of the core is used to inform the low-order thermal-hydraulic modeling with power distribution used to provide temperature feedback for neutronic calculations; the model is also capable of coupling with burnup calculations and pebble movement through the core.

3.2 Overview of VSOP Computer Code System

VSOP [4] is a computer code system for the comprehensive numerical simulation of an HTGR with spherical fuel pebbles. The application of the code includes the processing of cross-sections, the set-up of the reactor geometry and the fuel element (pebble), neutron spectrum evaluation, neutron diffusion calculation, fuel burnup, fuel shuffling, reactor control, and thermal hydraulics. The neutronic calculations can be performed in up to three dimensions. Thermal hydraulics is restricted to pebble bed HTGRs in two spatial dimensions.

VSOP [4] enables the user to follow the reactor life from the initial core toward the equilibrium core. Repeated calculation of the different physics features ensures consistency in their feedback during the proceeding burnup, the simulation of the fuel shuffling, and variations of the core power rating. Temperature transients can be followed by performing a quasi-static nuclear evaluation in parallel. A detailed power history of the fuel pebbles is used for the calculation of their individual decay power. Reprocessing and closure of the fuel cycle can be simulated under consistent control of the mass flow of the fuel, including the isotopic decay during periods of intermediate storage. As part of the burnup calculation, the code determines the impact from the most significant minor actinides on the physics of the reactor and the characteristics of spent fuel.

The specific applications of VSOP [4] at X-energy include:

- Reactor core steady-state design analysis
- 100% nominal full power equilibrium core analysis
- Initial start-up and approach to equilibrium core analysis

- Low power operation
- Load-follow maneuvering
- Reactivity control system requirements (e.g., shutdown margins)
- Providing input parameters to support the safety analysis
- Other operational transients that can be simulated with a quasi-static manner (i.e., slow transients that do not require modeling of the delayed neutrons and do not include gas dynamics)
- Tool for validation purposes and to perform research and development in aspects that involve, for example, advanced fuel cycle behavior

The input parameters used in support of the safety analysis includes the following items:

- Reactivity coefficients:
  - Fuel temperature coefficient
  - Moderator temperature coefficient
  - Reflector temperature coefficient
- Xenon feedback coefficients
- Control and shutdown element (rod) worth:
  - Integral worth
  - Differential worth
- Power distribution:
  - Peaking factor
  - Axial and radial power profile
- Kinetics parameters:
  - Delayed neutron fractions
  - Delayed neutron decay constants
  - Neutron mean generation time

3.2.1 VSOP Analysis Flow

The simplified calculation flow of VSOP [4] is included in Figure 5. The calculation flow accomplishes the following major activities:

- Generation of cross-section data including resonance integrals and neutron escape probabilities
- Based on user input, the generation of the neutronic and hydraulic computation mesh (this includes the core, reflector, control rods, etc.)
- Generation of few broad energy group cross-sections from a large number of energy groups by employing neutron spectrum calculations
- Determination of flux and power in the core, including the thermal-hydraulic feedback
- Advance the computation by updating burnups and composition for each mesh
- Continue to the next time step by updating the few broad energy group cross-sections with new isotopic, temperature, and feedback information; then reperforming the steps above

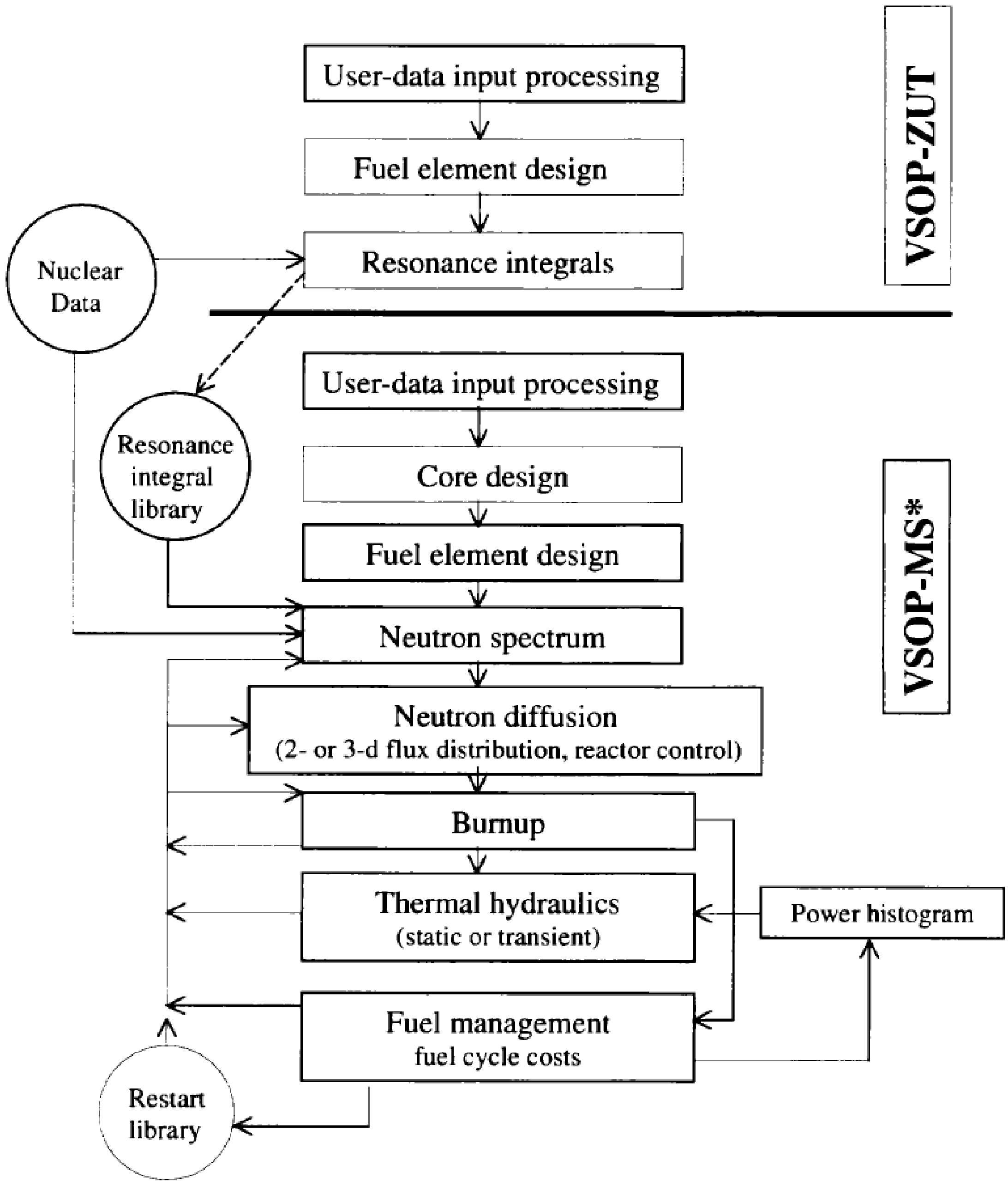

Figure 5: VSOP Program Flow

3.2.2 Cross-Section Libraries

VSOP [4] uses two libraries to encompass the entire neutron energy range. The first library is a 68-energy group structure ranging from 10 Mev to 0.414 eV. The second library is a thermal library with a 30-energy group structure ranging from 2.05 to 10^{-5} eV. The libraries contain 190 isotopes with their corresponding cross-sections. Out of the 190 isotopes, 28 are the heavy metal isotopes including thorium, protactinium, uranium, neptunium, plutonium, americium, and curium elements. In addition, the thermal library contains the scattering kernels for graphite, hydrogen, and oxygen as a function of temperature. The data for the libraries have been derived from the evaluated nuclear data files ENDF/B-V and JEF-1 using a neutron spectrum corresponding to a high-temperature gas-cooled reactor. These libraries are not required to be regenerated and with a total of 98 energy groups are the starting point for the VSOP [4] calculations.

Two other data sets are required for each fuel type. These are the resonance integrals and the escape probabilities. X-energy is planning to use the fuel type as described in Section 2.3 [[

]] ^{P}. Data sets are generated for each of these enrichments.

3.2.2.1 Resonance Integrals

For the resonance absorber isotopes, Th-232, U-238, Pu-240, and Pu-242, the resonance integrals are evaluated for a given isotopic concentration for the fuel type used in the analysis model, and at different temperatures of the respective absorber materials. Normally, two different sets of temperature dependent cross-sections are generated and used for each resonance absorber, both representing different absorber concentrations. These two concentrations represent [[

]] ^{P}. The code then first constructs new resonance cross-sections for these two [[ ]] ^{P} by interpolation between the values for different temperatures according to the calculated fuel temperature in each spectrum zone. It then determines the final cross-sections by interpolation between these two sets for the [[

]] ^{P}

Resonance integrals are calculated for each of the 68-energy groups. Cell calculations are performed for a predefined number of spectrum zones. The data is stored with the background absorption cross-sections of the 68-energy group library.

The resonance integral calculation is made for a homogeneous distribution of the resonance absorber in the finite volume of a TRISO particle. The transport equation is solved with a fine group structure over the energy range of each resonance. The code performs a direct numerical solution of the integral equation for the average flux in the absorber and obviates the necessity of choosing between the narrow and wide resonance approximations. The calculations include Doppler broadening, scattering and the $E^{-1/2}$ factor in the absorption cross section. The unresolved resonances are calculated in the narrow resonance approximation with consideration of the Porter-Thomas distribution of neutron widths.

3.2.2.2 Neutron Escape Probabilities

The geometric escape probability is defined as the probability, P(E), of a neutron moderated in an absorber zone to the energy level E, missing its next interaction in the same or another absorber zone. The probability for neutron reaction within a TRISO coated particle is determined by the geometric layout provided that the mean free path length, $1/\Sigma_1(E)$, does not significantly exceed the coated particle kernel inner radius r_1. If this criterion is not met, homogenizing over the particle leads to incorrect reaction rates. It is therefore necessary to derive substitute cross-sections in support of the calculated geometric escape probability $P(E)$.

A neutron flight path is considered to enter the region with TRISO coated particles with random angle of entry. The average distance between any two TRISO coated particles within the neutron flight path in a particle region with density N is set equal to L. This is equivalent to a neutron traversing any homogeneous medium for determining the probability of a singular TRISO coated particle being hit by that neutron. This factor ignores any correlation to the location of neighboring particles and is justified when averaged over many particles in a region.

The averaged length L is derived by considering the probability that the cross-section of a coated particle remains within dx of the flight path of a neutron. Then

$$\frac{1}{L}dx = r_2^2 \pi N dx \tag{1}$$

Where r_2^2 is the outer radius of a coated particle. The density N of coated particles per cm^3 refers to the filling factor f given by

$$f = \frac{4\pi}{3} r_2^3 N \tag{2}$$

Thus

$$L = \frac{4r_2}{3f} \tag{3}$$

The probability that a neutron will travel a distance L without any interaction is equal to the probability that a TRISO coated particle is crossed in addition to the graphite region in between the coated particles. This probability, denoted by W_{8c} is given by

[[ ]] P (4)

Where Σ_3^* is an updated cross-section. The total probability of n pieces with length L flying through the region without interaction is subsequently defined by [[ ]] P. From this, Σ_3^* is suitable for characterizing the continuous medium replacing the assumption of a heterogenous region. There is a considerable difference between the fuel in the TRISO-coated particle cross-sections, Σ_1, and the coatings of the TRISO-coated particle, Σ_2. Therefore, Σ_3^* deviates considerably from an averaged cross-section Σ_3 and adjustment factors are appropriately included. With the adjusted Σ_3^* cross-section, the probability W_{8c} is calculated.

Similarly, W_{71c}, is defined as the probability of an interaction within the fuel in a TRISO-coated particle due to a randomly penetrating neutron. Furthermore, W_{72c} is defined as the probability of an interaction in the graphite region. Then, the following relations is developed:

[[ ]] P (5)

Then, $1 - W_{8c}$ is the probability that an interaction will occur during flight of a neutron. This interaction is taking place within the fuel in the TRISO-coated particle with a probability of [[ ]] P, while [[ ]] P will be the probability of interaction within the graphite zone. Based on these probabilities, definitions, and adapted cross-sections for the interactions within the fuel in the TRISO-coated particle and graphite material are defined, respectively as

[[ ]] P (6)

and

[[ ]] P (7)

The calculation of interactions is explained by the sinew lengths which depict the neutron path of flight through the individual material zones with angle of entry ϑ, as represented in Figure 6. If $sin^2\vartheta = u$, then the following relationship holds:

$$l_1 = r_2 \left[\sqrt{1-u} - \sqrt{\left(\frac{r_1}{r_2}\right)^2 - u} \right],$$

$l_2 - l_1 = 2r_2\sqrt{\left(\frac{r_1}{r_2}\right)^2 - u},$

$l_3 = 2r_2\sqrt{1-u},$

$\lambda - l_0 = r_2\left[\frac{2}{3f} - \sqrt{1-u}\right]$, and

$sin^2\vartheta_0 = u_0 = \left(\frac{r_1}{r_2}\right)^2.$

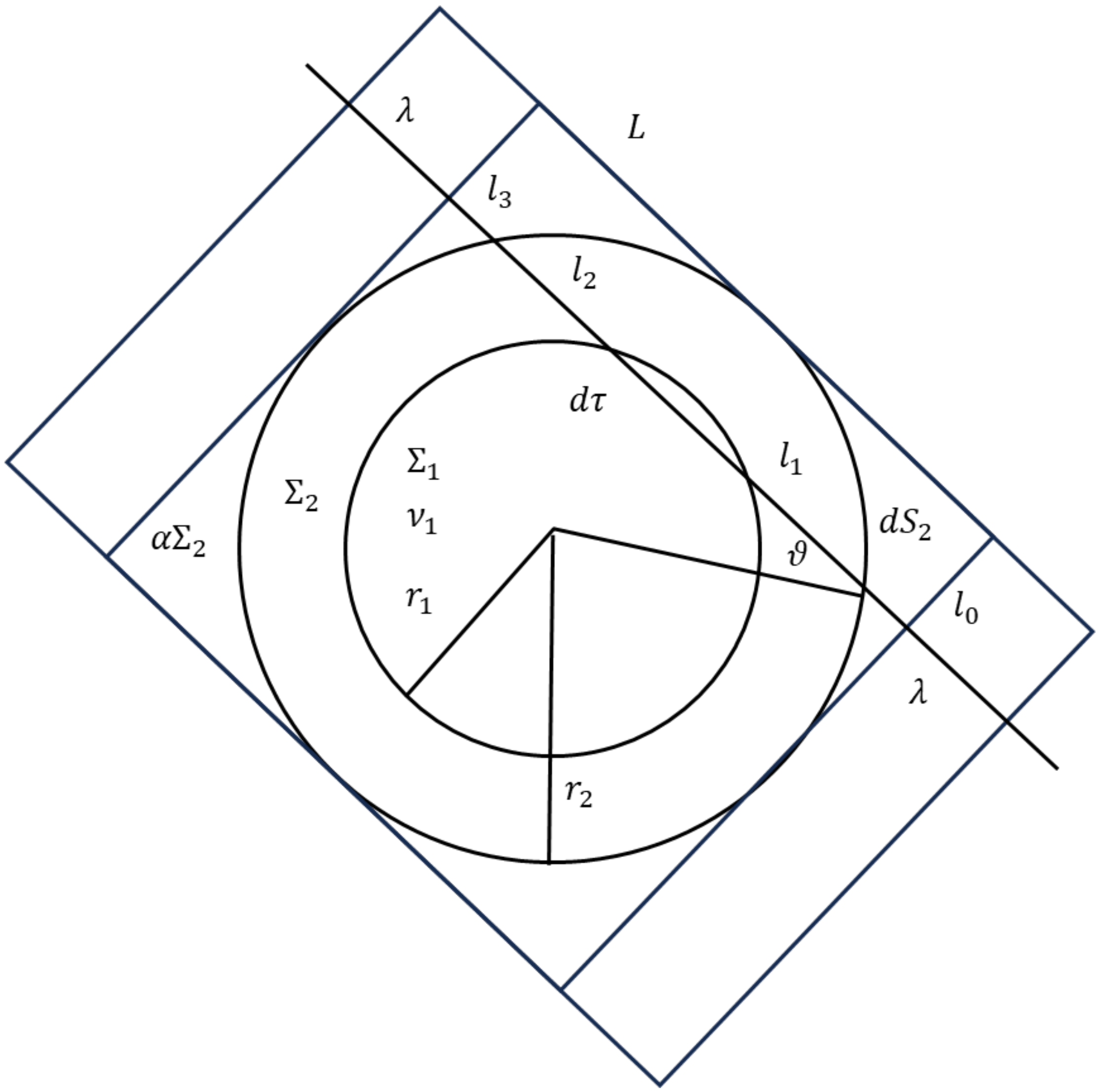

Figure 6: Calculational Model for the TRISO Coated Particle

Letting $\nu = \left(\frac{r_2}{r_1}\right)^2 . u$, then the probabilities can be calculated as follows:

[[

]] P (8)

[[

]] P (9)

[[ ]] P (10)

The discussion above applies to the TRISO-coated particles; a similar approach is used for the fuel pebbles. In Figure 7 the arrows indicate the various possibilities that exist for a neutron to experience a reaction in a moderation zone. All these possibilities are embedded in the calculation of P(E). In the case of coated particles inside a fuel pebble, the absorber lump is the inner kernel of a representative coated particle. Because of the small particle size (less than 1 mm in diameter in the case of the Xe-100 design), the escape probability P(E) is close to 1, even for neutrons with energy close to the peak of strong resonances. Neutrons can travel through many coated particles without any collision, whether through the coatings or streaming through the kernels. It can meet the boundary of the fuel matrix, pass through the outer shell of the fuel pebble, enter another matrix, and undergo collision in any of its coated particles or somewhere between them. For such double-heterogenous composition of the absorber lumps it is easier to determine the escape probability explicitly than to derive Dancoff factors in the usual way. Therefore, in VSOP [4], the escape probability P(E) is directly evaluated by a numerical method. This is done by an explicit calculation of W_v, the partial escape probabilities for each interaction that depends on the direction of flight of the neutron. Like the coated particle structure in the fuel pebble, a distribution for a random angle of entry is assumed in a pebble bed for the transfer from one fuel pebble to neighboring pebbles.

The partial escape probabilities W_v, indicated in Figure 7, are defined as:

- W_1 = the probability that a neutron born within the absorber zone of a coated particle will have its next reaction in the graphite region of the same coated particle. Apart from the graphite shell, a reaction within a portion of the matrix in between coated particles is included.
- W_2 = the probability that a neutron will leave a coated particle and the adjoining graphite region without an interaction.
- W_3 = the probability that a neutron that has left a coated particle has its next interaction in the graphite region of another coated particle within the same fuel pebble. An average value of all possible positions as to the originating coated particle is possible.
- W_4 = the probability that a neutron as mentioned in W_3 has its next interaction within the fuel free zone of the fuel pebble.
- W_5 = the probability that the neutron leaves the fuel pebble without any interaction.
- W_6 = the probability that a neutron coming from a neighboring fuel pebble with random angular distribution of entry has an interaction in the graphite region of a coated particle of that fuel pebble.
- W_7 = the probability that a neutron as mentioned in W_6 has its interaction in the fuel free zone of the fuel pebble.
- W_8 = probability that the neutron enters and leaves the fuel pebble without any interaction.

If the pebble bed is filled with a partial loading “h” of graphite pebbles with no fuel (i.e., blank pebbles), then W_8 constitutes the probabilities, W_{8a}, the portion of absorber pebbles, and W_{8g} the portion of graphite pebbles. This is similarly applicable to W_7 and W_6. Then the following relationships could be formulated:

[[

]] P

The geometric escape probability is then formulated based on the W_v as follows:

$$P€ = W_1 + W_2 * (W_3 + W_4) + W_2 * W_5 * (W_6 + W_7) / (1 - W_8) \quad (11)$$

Here the first sum refers to the interaction in the originating kernel, while the second refers to the originating pebble. The third aspect denotes the probability of the neutron exiting the pebble (W_2 * W_5), followed by the possibility of zero or more pebbles being penetrated without an interaction (1 / (1 - W_8)). Lastly an interaction occurs within a pebble in the graphite region (W_6 + W_7).

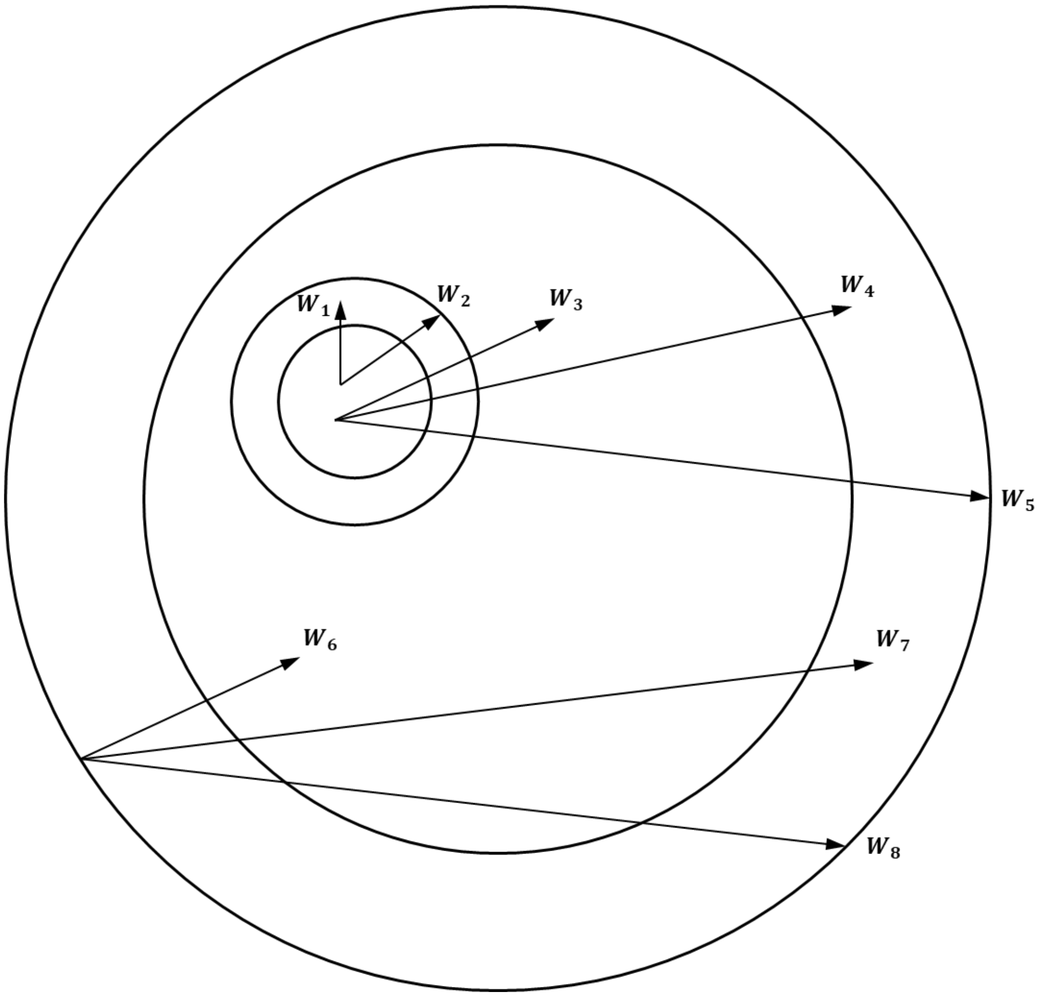

Figure 7: Partial Escape Probabilities W_v

Like the TRISO coated particles, a calculation model for the fuel pebble is defined and presented in Figure 8.

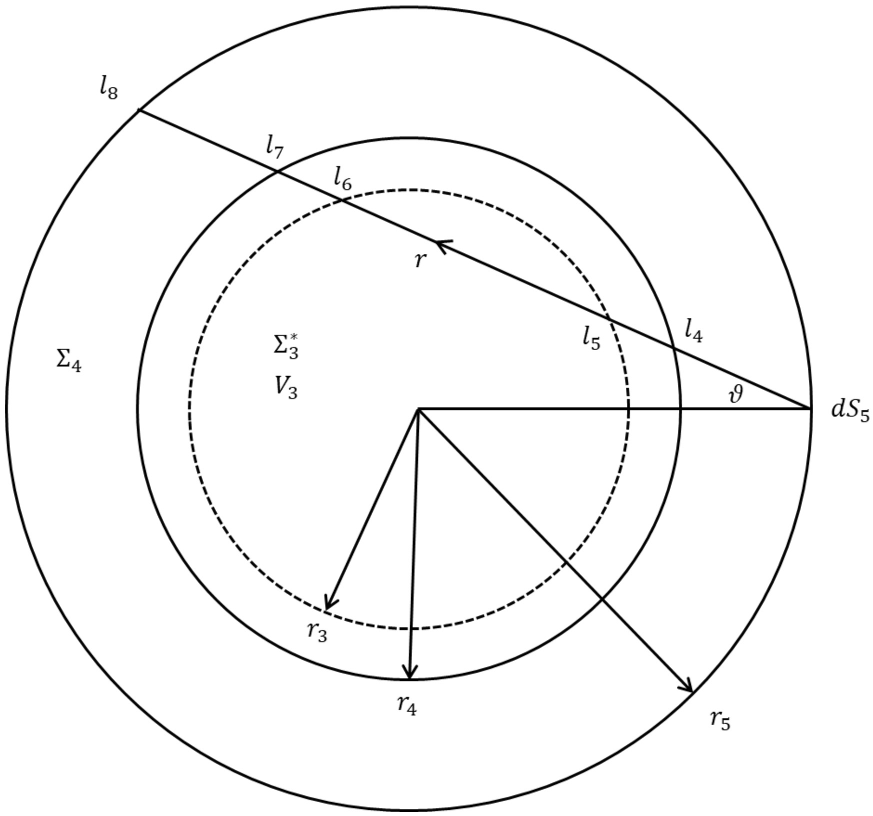

Figure 8: Wv Calculational Model for Fuel Pebble

With $u = sin^2\vartheta$ and $r_3 = r_4 - r_2$

$$l_4 = r_5\left[\sqrt{1-u} - \sqrt{\left(\frac{r_4}{r_5}\right)^2 - u}\right],$$

$$l_5 = r_5\left[\sqrt{1-u} - \sqrt{\left(\frac{r_3}{r_5}\right)^2 - u}\right],$$

$$l_6 = r_5\left[\sqrt{1-u} + \sqrt{\left(\frac{r_3}{r_5}\right)^2 - u}\right],$$

$$l_7 = r_5\left[\sqrt{1-u} + \sqrt{\left(\frac{r_4}{r_5}\right)^2 - u}\right],$$

$$l_8 = 2r_5\sqrt{1-u},$$

Notice that Σ_4 represent the cross-section of the fuel free zone of the fuel pebble. Then the probabilities are determined as follows:

[[ ]] P (12)

[[

]] P (13)

[[ ]]P

(14)

[[

]] P (15)

[[ ]] P

(16)

[[

]] P (17)

[[ ]] P (18)

Σ_5 is the total cross-section of graphite pebbles (blank pebbles). The W_4, W_{7a}, and W_{7g} can be calculated from the relationships:

[[ ]] P (19)

[[ ]] P

(20)

[[ ]] P (21)

Some of the above integrals can be performed analytically, but most are performed numerically. At this point in the calculation flow, VSOP [4] has the cross-section libraries encompassing 98-energy groups and the fuel type specific resonance integrals and collision probabilities for each fuel type.

3.2.3 Core Design

VSOP [4] can perform the core design calculations in 2 or 3 dimensions, however the Xe-100 reactor core design only uses the 2-dimensional (RZ) model. Based on the fueling configuration, the Xe-100 axial core model is subdivided into five radial pebble flow channels, numbered 1 through 5 going from left to right (center to edge of the core adjacent to the reflector wall). Each of the flow channels is subdivided in calculation sub-units, called "layers", to simulate the effect of the pebble axial flow velocities in each channel. The pebbles move at different velocities, with pebbles towards the center moving faster than pebbles closer to the reflector sides. These equal volume sub-units correspond to a "region", or a spectrum zone within the core. The pebbles in the core undergo an average of six fuel passes before being discarded, therefore the regions inside the core are in turn subdivided into six "batches" each to represent this six-pass fueling scheme. The isotopic concentration in these regions is used to calculate the spectrum and subsequently used in the determination of the broad group cross-section (see Section 3.2.4). A typical flow channel and region configuration is presented in Figure 9.

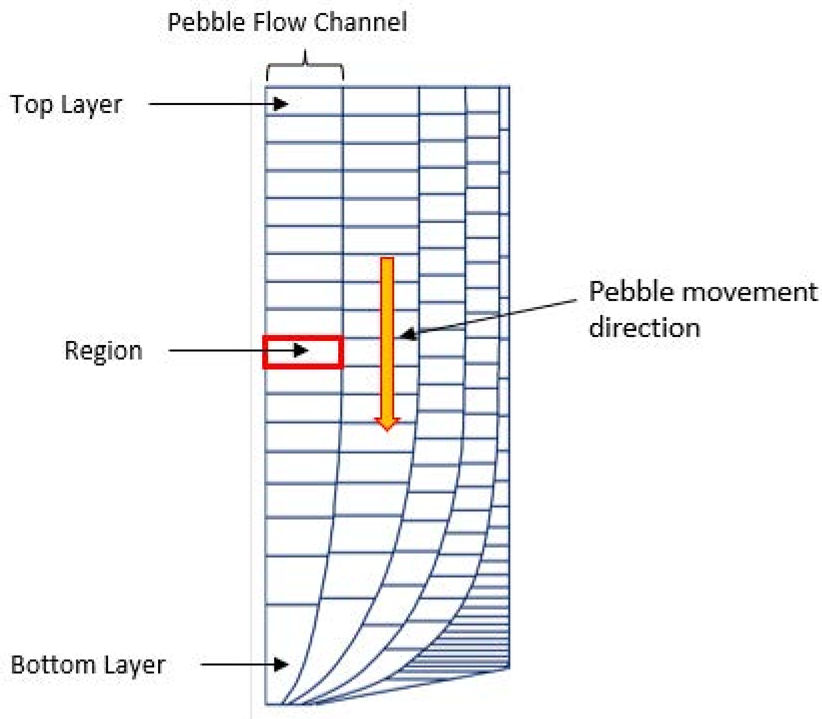

Figure 9: Typical Flow Channel and Region Configuration

The flow channel and region configuration are superimposed on a neutronic mesh. The neutronic mesh represents a finer mesh for the finite difference solution of the diffusion equation (see Section 3.2.5). The mesh for neutronic purposes includes the core, radial graphite reflector, helium gas space at the top of the core, and the top and bottom graphite reflectors.

In the mesh pattern the basic mesh unit comprises a predefined reactor material composition and is named a “batch”. The reactor core region is subdivided into batches, which are all filled with the fuel material. A batch represents pebbles from a given pass through the core, and a region contains pebbles from six different batches. The outer lying regions of the reactor comprises the reflector material, vessel material, void regions, etc.

According to this discrete mesh pattern the simulation will provide batch-wise data for the burnup, fuel shuffling, and the decay heat production parameters during steady-state and quasi-steady-state transients. A typical neutronics mesh is included in the Figure 10.

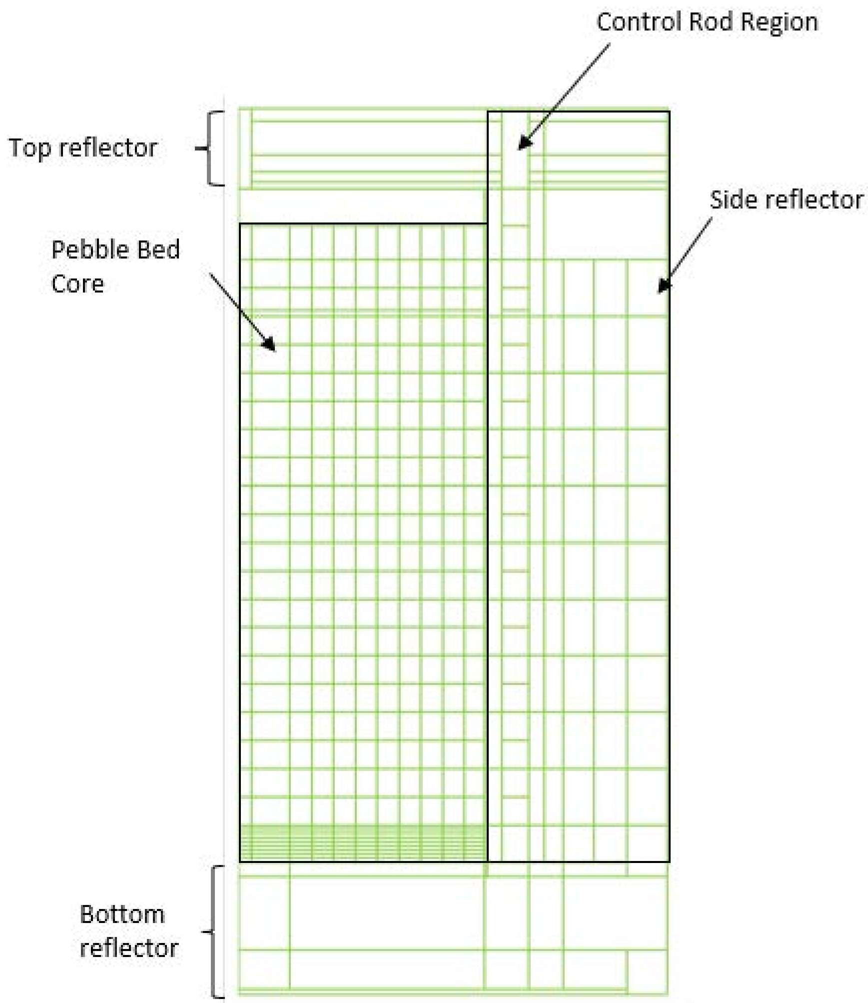

Figure 10: Typical Neutronics Mesh

3.2.4 Neutron Spectrum and Determination of Broad Group Cross-Sections

Assuming a space and energy dependent cell calculation, the reaction rate of any nuclide in any spectrum zone per volume (V_0) of the cell is given by,

$$R = \sum_{g=1}^{NG} \sigma_g \cdot SC_g \cdot \sum_{k=1}^{NK} N_k \cdot V_k \cdot \Phi_{kg} \tag{22}$$

Where:

> g, NG are the energy groups of the cross-section library
>
> k, NK are the cell zones in the model
>
> σ_g, SC_g cross-section and corresponding self-shielding factor
>
> V_k volume of cell zone k
>
> ϕ_{kg} neutron flux

The neutron reaction rate per cell volume can be described in terms of the average cell flux ϕ_{0g}:

$$R = \sum_{g=1}^{NG} \sigma_g \cdot SC_g \cdot N_0 \cdot V_0 \cdot \phi_{0g} \cdot \sum_{k=1}^{NK} \frac{N_k \cdot V_k \cdot \phi_{kg}}{N_0 \cdot V_0 \cdot \phi_{0g} \cdot} \tag{23}$$

with the following cell zone averaging applied

$$V_0 = \sum_{k=1}^{NK} V_k \qquad N_0 = \sum_{k=1}^{NK} N_k \cdot \frac{V_k}{V_0} \qquad \phi_{0g} = \sum_{k=1}^{NK} \phi_{kg} \cdot \frac{V_k}{V_0}$$

With the definition of the neutron self-shielding factors of the different cell zones

$$SF_{kg} = \frac{\phi_{kg}}{\phi_{0g}}$$

the reaction rate can be written in the form

$$R = \sum_{g=1}^{NG} \sigma_g^* \cdot N_0 \cdot V_0 \cdot \phi_{0g}$$

where the cross-section is modified by the self-shielding factors *SC* and *SF*

$$\sigma_g^* = \sigma_g \cdot SC_g \cdot \sum_{k=1}^{NK} \frac{N_k \cdot V_k}{N_0 \cdot V_0} \cdot SF_{kg} \tag{24}$$

The self-shielding factors represent parameters in the presence of a strong absorber, other than the fuel pebbles. Based on the design of the Xe-100 core and core components, these factors are set to [[ ]] P. These modified cross-sections σ^*_g are applied in the spectrum calculation and used to collapse the cross-section to form the broad group cross-sections which are used in the diffusion and burnup calculations.

For pebble bed HTGRs, four broad energy groups have proven to be adequate to perform the core systems calculations. The energy groups are:

- A thermal energy group between 0 to 1.86 eV,
- Two epithermal groups with energies ranging from 1.86 eV to 29.0 eV and 29.0 eV to 1.11 MeV, and
- A fast energy group with energies between 1.11 Mev and 10 MeV.

The 4-energy broad group cross-sections are determined from the 98-energy group cross-section by the equivalence theory as follows:

$$\sigma_{a,g} = \frac{\int_{E_g}^{E_{g-1}} \sigma_a(E)\phi(E)dE}{\int_{E_g}^{E_{g-1}} \phi(E)dE} \tag{25}$$

Where

$\sigma_a(E)$ is the microscopic cross-section of the continuous energy variable *E*, and

$\phi(E)$ is the scalar neutron flux spectrum.

Because the flux spectrum is not initially known, an approximate spectrum is determined using the collision probabilities presented above. Subsequent calculations use previous results as the starting values for the spectrum solution. Note that the flux spectrum and determination of the broad group cross-section are performed after each time step since there is a change in the isotopic compositions of the neutronic mesh.

3.2.5 Neutron Diffusion (Core Calculations)

Once the broad energy group cross-sections are calculated, the core flux and power distributions are determined using the diffusion equation. The following vector form of the diffusion equation is employed:

$$-\vec{\nabla} D(\vec{r},E)\vec{\nabla}\Phi(\vec{r},E) + \left(\Sigma_a(\vec{r},E) + \Sigma_s(\vec{r},E)\right)\Phi = \int_{E'}\left(\Sigma_s(\vec{r},E'\rightarrow E) + \frac{\chi_E\left(\nu\Sigma_f(\vec{r},E)\right)}{k_{eff}}\right)\Phi(\vec{r},E)dE' \tag{26}$$

Where

$D(\vec{r},E)$ = diffusion coefficient

$\Sigma_a(\vec{r}, E)$ = absorption cross-section

$\Sigma_s(\vec{r}, E)$ = scattering cross-section in the specific energy group

$\Sigma_s(\vec{r}, E' \rightarrow E)$ = cross-section for in-scattering into the specific energy group

$\chi_E\left(\nu\Sigma_f(\vec{r}, E)\right)$ = distribution function for the source neutrons (dependent on the production cross-section $\nu\Sigma_f$)

k_{eff} = the effective multiplication factor

The diffusion equation is solved using a finite-difference solution with temperature feedback. The following figure presents a representative fast and thermal flux for the Xe-100 design core.

[[

]] P

Figure 11: Xe-100 200 MWt Radial Flux Distribution

3.2.6 Modeling of Neutron Absorbers (Control Rods)

The diffusion theory has difficulties with treating the regions with strong neutron absorbers such as the control rods located in the side reflector in the case of Xe-100 design. Inside and in close proximity of such regions, the diffusion theory is not valid and therefore a special treatment is needed when modeling such regions in diffusion theory-based codes.

For the graphite moderated systems like HTGRs, Method of Equivalent Cross Sections (MECS) were adapted and used for the design and evaluation of the German HTR-Modul pebble bed reactor [32]. This method has been used previously for the evaluation of the ASTRA critical facility and shown good comparison with the experiments [33]. The principle in MECS is to model the absorber and its environment in transport theory (S-N) and then extract the transport corrected cross sections and diffusion parameters that will represent the absorber region accurately in subsequent 3D diffusion calculations. An equivalent B^{10} concentration is then used in the 2D model as a gray curtain that equates the total worth of the neutron absorbers previously calculated with 3D model.

The MECS methodology is based on some general assumptions, one of which is the assumption of flux-equivalence at points of equal distance from the absorber region surface independent of the absorber geometry since the transport calculation is normally performed in one dimensional geometry. Therefore, the azimuthal non-isotropy effects in the R-ϕ plane related to geometry effects (of either the absorber region or the overall reactor geometry) cannot be accounted for. This might be overcome by two-dimensional transport solutions.

In Xe-100 design, instead of using MECS methodology, a full core 3D Monte Carlo (MCNP) model is used for calculating the worth of the control rods at equilibrium core conditions. And an equivalent B^{10} concentration is used in a VSOP 2D model that equates the rod worths calculated by MCNP model. This methodology replaces the transport and 3D diffusion calculations and removes the assumptions that are required in case of MECS methodology.

3.2.7 Burn-Up Calculations

The burn-up calculation is performed for the 28 heavy metal isotopes in every mesh within the core. The simulation of the fuel burn-up is a combination of the simulation of the fuel shuffling, the evaluation of the space and energy dependent neutron flux, and the resulting local depletion and nuclides concentration. Burnup cycles are defined for pre-selected time periods. Each burnup cycle is subdivided into multiple time steps during which a diffusion and spectrum calculation are performed. During each time step the following results are generated:

I. Flux and power distribution,
II. Total nuclide concentration in every region, and
III. Total weight of all heavy metals and per region.

These results are used to determine the burnup for each mesh in the core. The burn-up is expressed in Fissions per Initial Metal Atoms (FIMA). This can be described as:

$$\mathrm{FIMA} = \frac{\sum_i N_i^0 - \sum N_i(t)}{\sum_i N_i^0} \tag{27}$$

Where

$\sum_i N_i^0$ = Sum of all heavy metal atoms before irradiation, and

$\sum N_i(t)$ = Sum of all heavy metal atoms at time t.

3.2.7.1 Fission Product Buildup and Decay

VSOP [4] tracks up to 44 fission product isotopic chains. There are 43 explicit fission product chains that were found to cover 98% of the fission product absorptions during the simulation of the HTR-MODUL [12]. The remaining absorption isotopes are addressed as part of a Cumulative Fission Product chain. This chain represents the sum of many low-absorbing fission products that are excluded from the explicit 43 chains.

The Xenon-135 (Xe-135) chain is the most important neutron poison because it has an extremely large thermal neutron absorption cross-section of about 2x10^6 barns, compared to about 500 barns for U-235 thermal fission cross-section. Xenon is a fission product that is formed directly by fission, as well as by β decay of the $^{135}Te \rightarrow {}^{135}I \rightarrow {}^{135}Xe$ chain. Xe-135 is removed by direct neutron capture as well as decay to the Cs-135 isotope. The production and decay are explicitly modeled.

3.2.8 Thermal Hydraulics

VSOP [4] determines the temperature of the fuel and the moderator averaged over the volumes of the cells and are used to adjust the spectrum and cross-sections, thus providing the feedback to the neutronic calculation. The calculation of the overall heat transmission is synthesized by the coupling of different equations, which represent conservation laws.

The conservation of mass of the cooling gas in quasi-static representation yields the mass flow vector $G = \rho_G \cdot \mathbf{v}$ over the circuit. It is given by

$$\nabla \rho_G \cdot \mathbf{v} = q \tag{28}$$

where

ρ_G = density of the cooling gas [kg/m^3]

$\mathbf{v}$ = velocity [m/s]

q = mass source rate density [kg/s/m^3]

The conservation of momentum quasi-static representation yields the pressure field p over the circuit. It is given by

$$\nabla p - \rho_G \cdot \mathbf{g} + \mathbf{R} = \mathbf{0} \tag{29}$$

where

ρ = static pressure

$\mathbf{g}$ = gravity

$\mathbf{R}$ = frictional force

Equation (29) gives the balance of the gradient of the pressure, the hydrostatic force of gravity, and the frictional force per unit volume. The spatial acceleration and inertia are neglected. The frictional force is given by

$$\mathbf{R} = \frac{\psi}{d} \cdot \frac{1-\varepsilon}{\varepsilon^3} \cdot \frac{|G|}{2\rho_G}\mathbf{G} \tag{30}$$

where

ψ = pressure loss coefficient for flow through pebble bed (given as a function of the Reynolds number)

d = pebble diameter

ε = pebble bed void fraction

The conservation law of the energy in quasi-static representation yields the gas temperature field T_G:

$$\nabla \lambda_G \nabla T_G - \nabla(\rho_G \cdot \mathbf{v} \cdot c_p \cdot T_G) + \alpha \cdot \frac{F}{V} \cdot (T - T_G) = 0 \tag{31}$$

where

c_p = gas specific heat capacity

λ_G = effective thermal conductivity of the gas due to dispersion

T = temperature of the solid, e.g. at the surface of the fuel elements (pebbles)

$\alpha \frac{F}{V}$ = coefficient of heat transition between the solid and the gas

In the above equation, the first term gives the heat transport in the gas by thermal conduction. The second term is the heat transport according to the mass flow of the gas. The third term is the heat source or sink due to the heat transition between the gas and the fuel pebbles. The compressive work term and the time dependent energy storage are neglected.

The conservation law of energy in the solid material is evaluated in the dynamic representation. It yields the temperature field *T* :

$$\rho \cdot c \cdot \frac{\partial T}{\partial t} = \nabla \lambda_{eff} \nabla T + \alpha (T_G - T) + Q \qquad (32)$$

Where

T = $T(\mathbf{r}, t)$ temperature of the solid, i.e. at the surface of the fuel pebbles, in reflectors, etc.

ρ = density of the solid

c = heat capacity

λ_{eff} = effective thermal conductivity, which includes thermal conduction and radiation

α = coefficient of heat transition between gas and solid

Q = $Q(\mathbf{r}, t)$ nuclear heat source

In equation (32), the time dependent change of the energy per volume results from the balance of the heat transport by thermal conduction (first term), from the heat sink due to the heat transition to the gas (second term), and from the heat source due to the nuclear power production and decay power (third term). The fuel pebble temperature distribution T_F is also given by the conservation law of energy in time dependent representation:

$$\rho \cdot c \cdot \frac{\partial T_F}{\partial t} = \nabla \lambda \cdot \nabla T_F + Q \qquad (33)$$

where *c* and λ are dependent on the local temperature T_F. At the surface of the fuel element, the temperature T_F is equal to *T* of equation (32) at the respective position in the reactor.

Under steady state condition, an iterative procedure is performed which yields a consistent solution for the temperatures of the solid and the gas. Under dynamic conditions the time dependent changes of *T* and T_F are explicitly determined. Here, the time dependent change of the heat source *Q* is also included which is due to given changes of the power of the isotopic decay power.

3.2.9 Decay Heat

VSOP tracks the fuel life history to calculate the decay heat, which is based on the German standard, DIN 25485 [21]. This standard is derived for pebble bed high temperature gas-cooled reactors with a low enriched non-recycled fuel cycle. It has been used internationally for pebble bed reactors and in many physics computer codes.

The standard takes in to account the composition and power of the fuel during operation by considering:

- The flow of the fuel pebbles through the different power regions of the reactor
- The possible change in total core power
- The production and utilization of fissile isotopes

These are applicable to and required for pebble bed reactors. These are all taken into consideration by dividing the operating time into time intervals with constant power and constant power contributions from the fissile isotopes, i.e., using the power histogram which, for the Xe-100, is calculated by VSOP.

DIN 25485 [21] standards consider contributions from:

- Fission products from fissions of the four isotopes ^{235}U, ^{238}U, ^{239}Pu and ^{241}Pu
- Actinides
- Isotopes resulting from neutron capture of fission products (the contribution of Cs-133 to Cs-134 is significant and it is treated separately)

3.2.10 Fuel Management

As described in Section 2.2, the fuel pebbles are introduced at the top of the core and move downward through the core until they exit at the bottom. Based on their burnup characteristics they are either returned to the top of the core or sent to be discharged. In the Xe-100 design a fuel pebble will pass on average six times through the core.

3.2.10.1 Pebble Flow

Pebble flow to VSOP is an input from STAR-CCM+ (Section 3.3). The fuel pebbles within the reactor move very slowly through the core during operation (on average, for Xe-100 design a given pebble will pass through the core in approximately half a year but there is considerable variance). The flow velocity of the pebbles is strongly influenced by the conical bottom reflector and wall effects (resistive forces at the wall are different than resistive forces in the main bed). The Xe-100 models the pebble core flow in five radial flow channels. Within each flow channel, the pebble velocity is viewed to be radially independent. Velocity in effect therefore means the velocity of the vertical components. Then, within each flow channel, the continuity equation holds:

$$M(r,z) = Q(r,z) \cdot v(r,z) = M(r), \quad (34)$$

where M = the volume flow

Q = the cross-sectional area, and

v = vertical velocity components.

The velocity of the fuel pebbles in these flow channels is determined by the method described in Section 3.3. For each time step, as the fuel pebbles flow in the vertical direction, the mesh composition changes, and the spectrum, flux, power, and temperature distribution are recomputed.

3.2.10.2 Pebble Shuffling

Fuel pebbles move axially within their respective channels and move to the next layer downward in each burnup time step (refer to discussion in Section 3.2.3 and Figure 9). When the pebbles reach the bottom layer, they are moved to one of several simulated storage boxes based on the number of passes through the core. Once a pebble has been returned to the top of the core, it is not possible to ascertain in what radial channel it will be located. For that reason, VSOP [4] volume averages the isotopic content, burnup, and the fast fluence values of the pebbles located in the storage box, and then the pebbles with their newly averaged composition are re-introduced at the top of the pebble bed to the next batch.

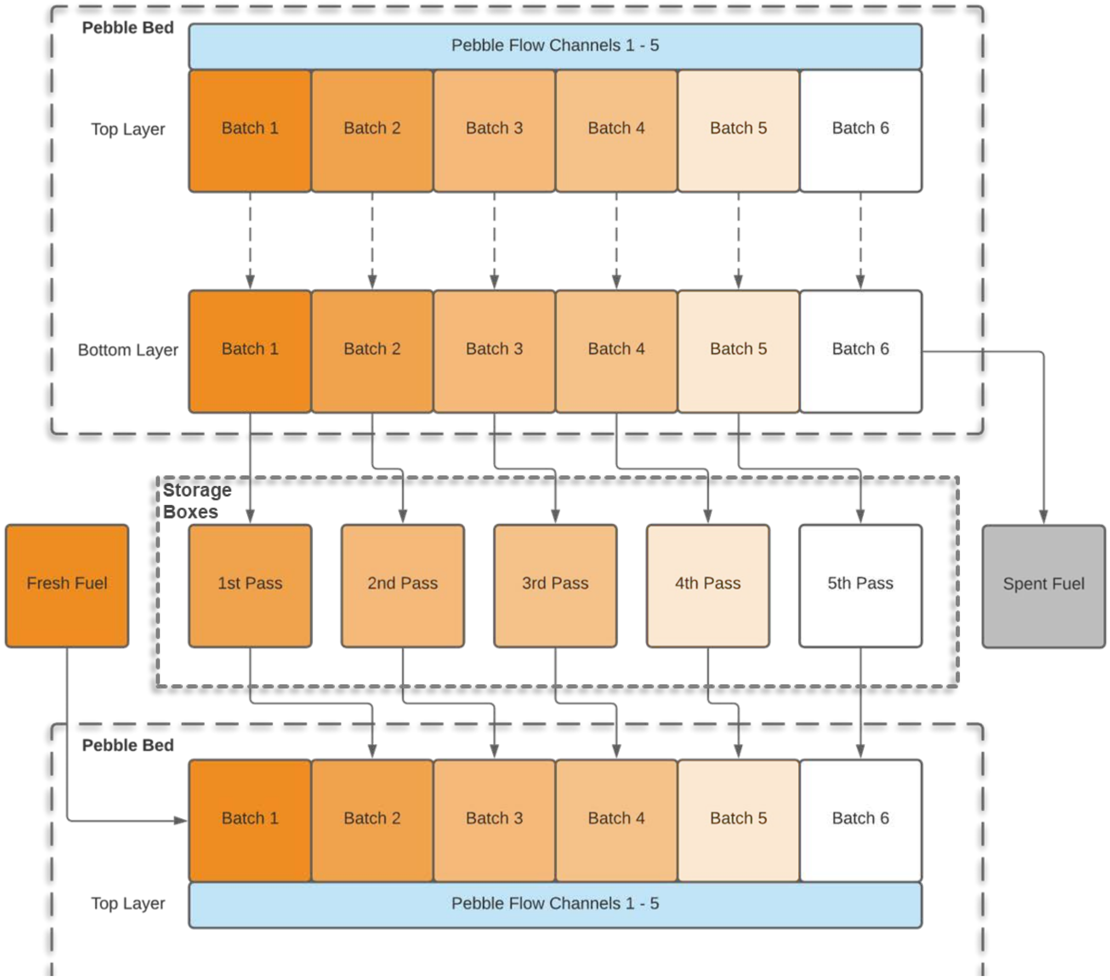

Figure 12: Fuel Shuffling Sequence

3.2.11 VSOP Calculation Capabilities

From the discussion above, VSOP [4] has the capability to determine the flux and power distribution for a startup, approach to an equilibrium core, and equilibrium core conditions. As part of these calculations, reactivity coefficients, control rod worth, and xenon feedback constants can be determined. An additional capability of VSOP [4] includes the data to generate the kinetics parameters required to support the safety analysis. These kinetics parameters include:

- Delayed neutron fractions
- Delayed neutron decay constants
- Neutron mean generation time

The delayed neutron fractions are given by

[[ ]]^P *(35)*

and the corresponding decay constants are

[[ ]]^P *(36)*

Where

l is the delayed group
m is the fissionable nuclide
β*m* is the total fraction of delayed neutrons from nuclide *m*
[[ ]]^P
λ is the decay constant for delayed neutron group *l* after fission in nuclide *m*

The neutron mean generation lifetime is determined as follows using the information developed from VSOP.

$$\boldsymbol{\Lambda} = \frac{\sum_g \frac{1}{V} \phi_g}{\sum_g \chi_g \nu \Sigma_{f,g} \phi_g} \qquad (37)$$

Where,

g is the neutron energy group
V is the neutron velocity
ϕ is the neutron flux
χ is the fission spectrum
ν is the average number of neutrons per fission
Σ_f is the fission cross-section

3.3 Overview of STAR-CCM+

The STAR-CCM+ [5] software package provides an environment in which detailed Computational Fluid Dynamics (CFD) simulations can be configured, executed, and interrogated. The software includes mathematical models for a wide range of relevant phenomena such as turbulence, heat transfer, and porous media. These phenomena are modeled by solving governing equations, from first principles, that approximate the behavior of physical systems.

While the code package has significant capabilities, the Xe-100 reactor core design only uses STAR-CCM+ [5] to determine the pebble flow characteristics through the core for specific radial flow channels as an input into the VSOP [4] code system. The following provides a summary of the functions and methods used in STAR-CCM+ [5].

3.3.1 Pebble Bed Flow Mechanics

Because pebble flow affects the core residence time of the pebbles, it has a direct impact on the reactivity and therefore core temperature and burnup. Factors that influence pebble movement can be summarized into three important concepts:

1) Core geometry:
    a) The physical geometry of the reflector encapsulating the pebbles determine how the pebbles propagate through the core.
    b) Geometric features such as wall-dimples and funnel angle all influence how pebbles move through the core.
    c) Three-dimensional Computer Aided Design (CAD) of the reflector geometry is used as input to Discrete Element Method (DEM) pebble flow analyses. DEM is an extension of the more general Lagrangian approach of modeling discrete particles.
2) Contacting pebbles:
    a) Pebble flow in the core is dependent on the physical interaction between contacting pebbles. As such, a DEM approach is used to model this interaction between pebbles in contact.
    b) DEM is a Lagrangian approach which allows for modeling of discrete elements and, in this case of the Xe-100's core, the discrete elements are spherical pebbles. Discrete elements (pebbles) in DEM modeling (1) have substance (mass), (2) cannot pass through walls or each other, and (3) can transfer momentum from one pebble to the next in a collision.
3) Contact characteristics:
    a) Because the DEM elements, or pebbles, come into contact, the properties of the materials coming into contact influence the way two pebbles react in a collision. These material properties that influence contact behavior are referred to as *contact characteristics*.
    b) Contact characteristics are (1) representative of the materials in contact, (2) typically obtained via empirical data, and (3) are incorporated into the DEM approach with a *contact model*.
    c) For the Xe-100's pebble flow analyses a *Hertz-Mindlin Contact Model* is used to model sliding friction and momentum transfer of contacts and collisions, respectively. This model takes two contact characteristic properties as input:
        i) Coefficient of Friction (COF), which represents the resistance to sliding for specific materials in contact.
        ii) Coefficient of Restitution (COF), which represents the amount of momentum transferred or lost in a collision of DEM elements (fuel pebbles). In other words, this portion of the Hertz-Mindlin contact model allows for the calculation of inelastic collisions.
    d) Similarly, for the Xe-100's pebble flow analyses a *Force Proportional Rolling Contact Model* is used to model the rolling friction of discrete elements in contact. This model accounts for the

impact that a discrete element's shape has on rolling. For example, spheres roll more freely than faceted polygonal shapes. This model takes one input:

i) Rolling resistance which, intuitively, is low for shapes that roll freely and high for shapes that have a high resistance to rolling. For the Xe-100's spherical pebbles, this value is low, as expected.

3.3.2 Hertz-Mindlin Contact Model

This section expands on the Hertz-Mindlin contact model as mentioned in point (3) of Section 3.3.1 above. This model incorporates the sliding behavior of materials in contact, and the momentum transfer between discrete elements (fuel pebbles) through a collision.

The Hertz-Mindlin formulation utilizes a spring-dashpot model. In this model, the spring generates a repulsive force, pushing particles apart, while the dashpot symbolizes viscous damping, and therefore allows modeling of inelastic collisions. At the point of contact, the forces are modeled by two spring-dashpot oscillators. There is a parallel linear spring-dashpot that models the normal force, and a parallel linear spring-dashpot in series with a slider, used to model the tangential direction of force. The springs model the elastic part of the phenomenon while the dashpot models the energy dissipation during the collision. See Figure 13 [5].

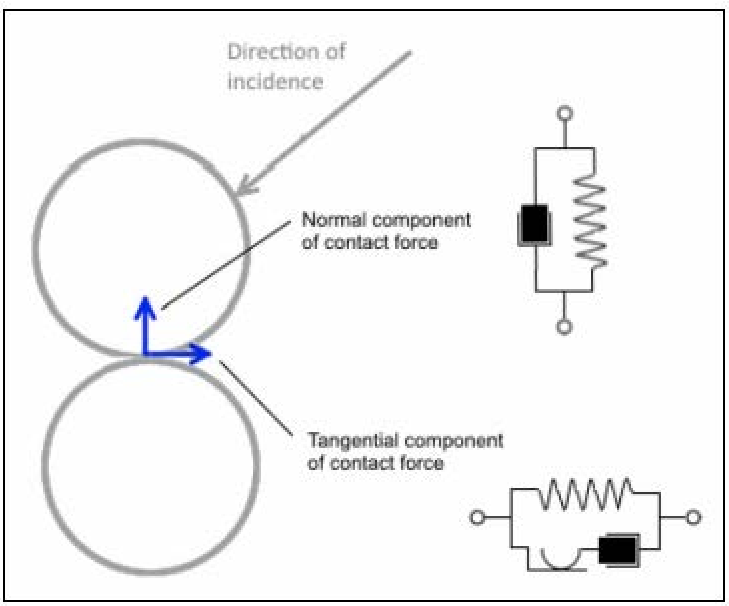

Figure 13: Spring-Dashpot Contact Representation

Contacts between fuel pebbles in the Xe-100 core are being modeled using the Hertz-Mindlin contact model. This is a variation of the non-linear spring-dashpot contact model which originates with Hertz-Mindlin contact theory. In this theory, the forces between two pebbles, A and B, are described by the following equations:

$$\boldsymbol{F}_{contact} = \boldsymbol{F}_n + \boldsymbol{F}_t \tag{38}$$

Where:

$\boldsymbol{F}_n$ is the magnitude of the normal component, and

$\boldsymbol{F}_t$ is the magnitude of the tangential component

The normal force is described by the following equation:

[[***]]***[P] *(39)*

Where:

d_n is the overlap in a soft contact model of the normal directions at the point of contact

v_n is the normal velocity component of the relative pebble surface velocity at the point of contact

K_n, the normal spring stiffness, is given by: [[ ]] *P*

- E_{eq} is the equivalent Young's modulus
- R_{eq} is the equivalent radius

N_n, the normal damping, is given by [[ ]] *P*

- M_{eq} is the equivalent particle mass
- $N_{n\,\mathrm{damp}}$ is the normal damping coefficient

The tangential force is described by the following equation:

[[***]]*** P *(40)*

Where:

d_t is the overlap in a soft contact model of the tangential directions at the point of contact

v_t is the tangential velocity component of the relative pebble surface velocity at the point of contact

K_t, the tangential spring stiffness, is given by: [[ ]]P

- G_{eq} is the equivalent shear modulus

N_t, the tangential damping, is given by [[ ]] P

- $N_{t\ \mathrm{damp}}$ is the tangential damping coefficient.

The rolling resistance of the pebbles is being modeled by the force proportional method. The method uses a coefficient of rolling resistance μ_r (also known as the coefficient of rolling friction). There is a moment due to the rolling resistance, which acts on the particle and is calculated by the following equation.

[[ ]] P **(41)**

Where:

μ_r is the coefficient of rolling resistance

$\boldsymbol{F_n}$ is the magnitude of the contact force

$\boldsymbol{r_c}$ is the position vector from the pebble centroid to the point of contact

$\boldsymbol{w_p}$ is the component of the pebble angular velocity which is parallel to the contact plane

Note that the brackets | | represent the scalar magnitude of the vector

3.3.3 Data Transferred to VSOP

A model of the Xe-100 core is developed using a DEM approach as described in the preceding sections. Each pebble is modeled as a spherical DEM element with mass and substance which cannot pass through walls or other elements. These DEM elements can come into contact with each other and the encapsulating reflector, which intrinsically accounts for geometric effects on pebble flow. Material specific contact characteristic properties are accounted for using Hertz-Mindlin and Force-Proportional Rolling contact resistance models.

This model thus predicts pebble movement through the core as pebbles are circulated through the core. Where 'circulation' refers to the process of removing the bottom-most pebbles from the core and adding new ones at the top. As pebbles move downward through the core towards where the bottom-most pebbles are removed, the DEM model calculates the path and time that each pebble takes. These paths are dependent on the factors discussed in Section 3.3.1 and are time-averaged to predict the expected pebble movement of the bed as a whole. Pebble flow paths, and residence times, as a function of location in the bed is transferred as input into the VSOP [4] code.

Predicting pebble flow behavior is primarily done to improve VSOP calculations by utilizing Xe-100 specific pebble flow lines as opposed to that from literature. However, scoping analyses have shown that retention time ratios, that is the ratio of pebbles' in-core time through the centerline vs. at the wall, has little impact on core safety limits.

4. Results from Core Physics Methods

This section provides results of typical calculations performed by VSOP [4] that support the safety analysis and demonstrates the capability to model important physical characteristics of the Xe-100 reactor. The VSOP [4] model used in this section corresponds to an equilibrium steady state configuration.

4.1 Reactivity Coefficients

The following table presents the fuel, moderator, and reflector temperature coefficient at 100% power. The results demonstrate an overall negative temperature coefficient for the Xe-100 core.

Table 2: Typical Temperature Coefficients at 100% Power

[[

]] P

4.2 Xenon Feedback Coefficient

The xenon feedback coefficient is determined by perturbing the xenon concentration and calculating the reactivity introduced by changes in the xenon concentration at different temperatures. As the average moderator temperature increases, the xenon feedback coefficient decreases, indicating that more neutron absorption by xenon occurs at lower temperatures than higher temperatures. The following table presents the xenon feedback coefficient versus temperature.

Table 3: Xenon Feedback Coefficient Versus Temperature

[[

]] P

4.3 Control and Shutdown Element Reactivity Worth

The following table and figure present a typical control and shutdown reactivity worth as a function of bank insertion. At equilibrium 100% nominal conditions, the control bank insertion depth is 174.9 cm below the bottom of the top reflector while the shutdown bank is at a fully withdrawn position located at the bottom of the top reflector. At a fully inserted position, the control bank is inserted to 7.2 m below the bottom of top reflector while the shutdown bank is inserted to 8.2 m below the bottom of top reflector.

Table 4: Typical Control and Shutdown Reactivity Worth

[[

]] P

[[

]] P

Figure 14: Typical Control and Shutdown Reactivity Worth

4.4 Core Power Distribution

A typical 100% radial power distribution is presented in the following figure. The power increases at the edge of the pebble bed core are due to the thermal neutrons reflected back to the core after they are thermalized in the reflector.

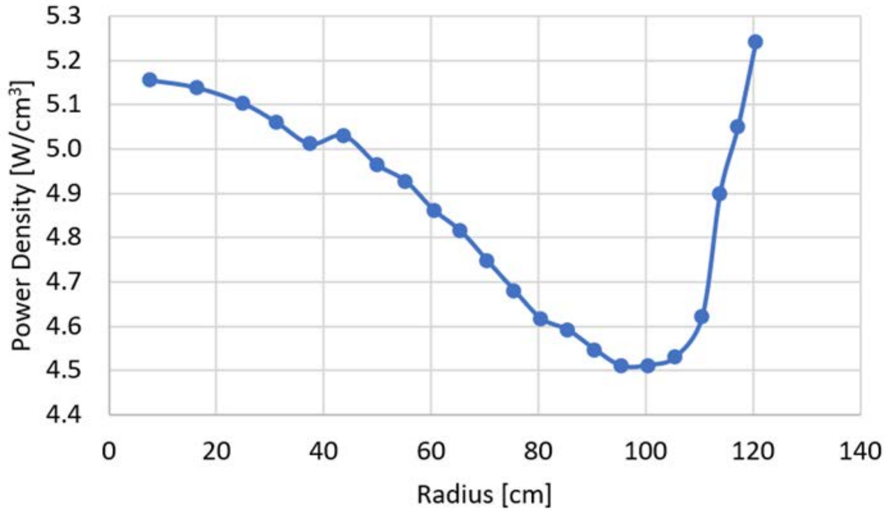

Figure 15: Typical 100% Power Radial Power Distribution

A typical axial power distribution at 100% power is presented in the following figure. It represents a top peaked power distribution due to the presence of fuel that is less depleted, and lower coolant temperature in these regions.

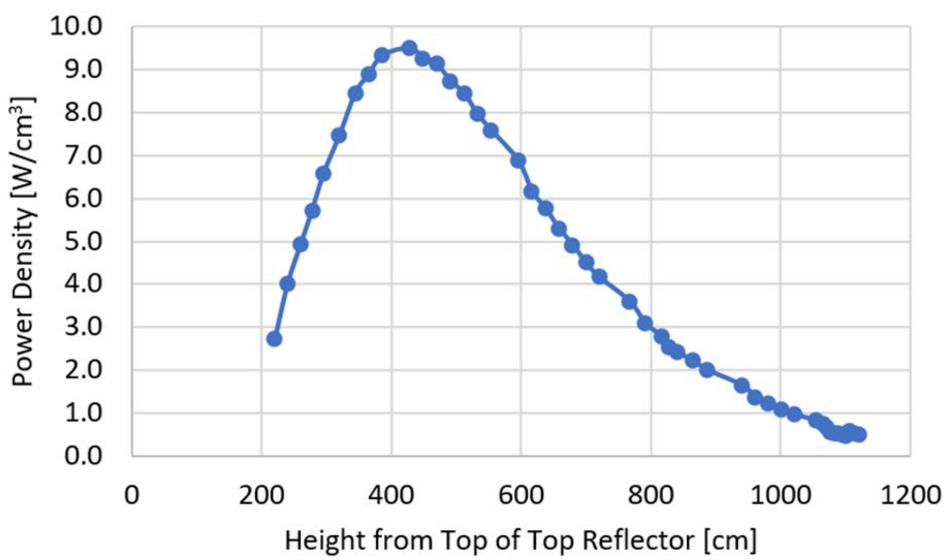

Figure 16: Typical 100% Power Axial Power Distribution

4.5 Kinetics Parameters

A representative six-group delayed neutron data for 100% power is presented in the following table. Using this data, a *βeff* of [[ ]] P is calculated.

Table 5: Six-Group Delayed Neutron Data for 100% Power

[[

]] P

4.6 STAR-CCM+ Input to VSOP

As discussed in Section 3.0., the only parameters that are calculated by STAR-CCM+ [5] are the pebble flow characteristic for each of the radial channels. A typical result for relative pebble velocity as function of radial position in the bed is presented in Table 6. Lower pebble velocities are expected at the interface between the core and the inner reflector.

Table 6: Typical STAR-CCM+ Relative Velocity for Each Radial Channel

[[

]] P

5. Code Validation

5.1 VSOP

5.1.1 VSOP Validation General Considerations

The validation plan for VSOP [8] is based on a comparison of VSOP produced results with existing experimental and operating data and comparison with results produced by other codes. The following studies have evaluated the use of experimental facilities to validate physics codes for phenomena relevant to HTGRs:

- ORNL - Relevant Advanced Reactor Benchmarks for Nuclear Data Assessment [15],
- ANL - Preliminary Assessment of Existing Experimental Data for Validation of Reactor Physics Codes and Data for Next Generation Nuclear Plant (NGNP) Design and Analysis [16],
- KAERI - Status of Experimental Data for the VHTR Core Design [17],
- IAEA - Evaluation of High-Temperature Gas Cooled Reactor Performance: Benchmark Analysis Related to the PBMR-400, PBMM, GT-MHR, HTR-10, and the ASTRA Critical Facility [18], and
- NEA – Experimental Facilities for Gas-Cooled Reactor Safety Studies [19].

X-energy's review of these studies identified that three experimental data sets from these facilities are applicable to the Xe-100 design. These facilities and associated experimental data sets are the HTR-10, ASTRA, and HTR-PROTEUS. These facilities/benchmarks are described and assessed in more detail in the following sections.

5.1.1.1 HTR-10

The HTR-10 is a 10 MWt high-temperature gas reactor with a pebble bed core that was designed, constructed, and operated by the Institute of Nuclear and New Energy Technology (INET).

The main design parameters of the HTR-10 are shown in Table 7 and the primary side schematic is shown in Figure 17. Data from this facility has been made publicly available through an IAEA benchmark exercise. Available data includes the following:

- Criticality Test – Criticality achieved without control rod inserted.
- Temperature Coefficient Test – Calculates keff at various temperatures without control rods inserted.
- Control Rod Worth Full Core Test – The reactivity worth of:
  - Ten fully inserted control rods, and
  - One fully inserted control rod.
- Normal Operation Test – The facility is operated at full power conditions
- Power Ascension Test – Increases the power from 30% full power to 100% full power

Table 7: HTR-10 Main Design Parameters

Parameter	Value
Reactor thermal power, MW	10
Primary helium pressure, MPa	3.0
Average helium temperature at reactor outlet, °C	700
Average helium temperature at reactor inlet, °C	250
Helium mass flow rate at full power, kg/s	4.32

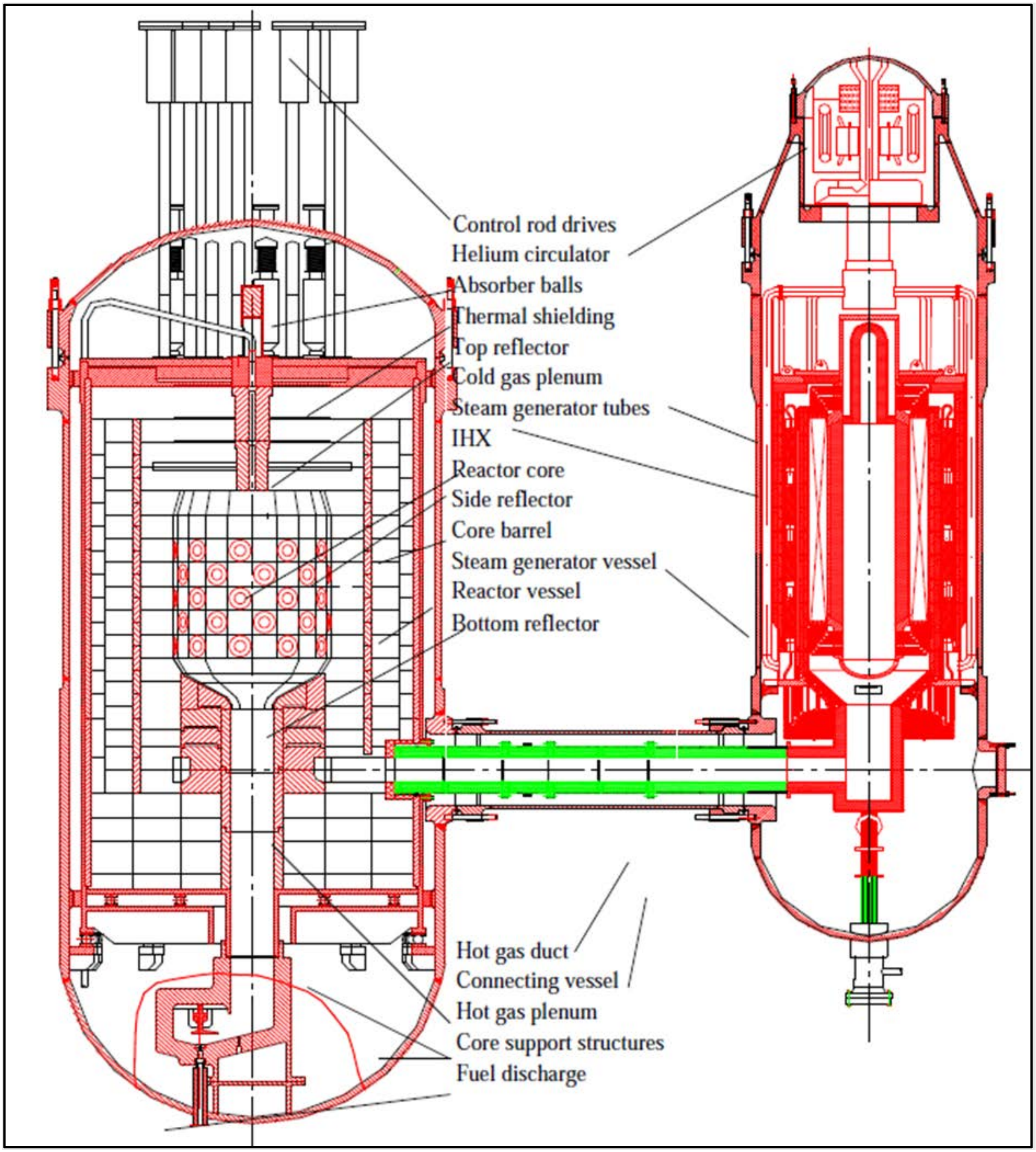

Figure 17: HTR-10 Primary System

5.1.1.2 ASTRA

The ASTRA critical facility at the Kurchatov Institute has been used for the experimental investigation of neutron-physical characteristics of HTGR reactors. The facility consists of an upright circular graphite cylinder (the side reflector) that encloses an octagon-shaped core region. Figure 18 shows a schematic view of the critical assembly cross-section and longitudinal section.

A considerable number of experiments investigating the high-temperature reactors have been performed at the ASTRA critical facility. The more recent experiments carried out at the ASTRA critical facility were intended for simulation of the high-temperature pebble bed modular reactor (PBMR) with the annular core that was being developed in South Africa.

Critical parameters of the basic configurations of the assemblies simulating the PBMR reactor are given in Table 8. Critical states of the assemblies were attained with control rods. Measurements of the critical states of the assemblies were performed with the accuracy of 0.0005 βeff.

Data obtained in the ASTRA facility can be used to compare measured and calculated values of:

1. Keff
2. Efficiency of control rods
3. Kinetic parameters

Table 8: Examples of the Core Configurations at the ASTRA Facility

Config.	Cross-Section	Core Height, m (Total number of FE)	Spherical Element (Fuel Pebble) Ratio in the core
1	Octagon, $Ø_{eff}$ = 1.8m	1.76 (23,600)	FE/AE=100/5
2	Circle, $Ø_{eff}$ = 0.938 m	3.02 (11,300)	FE/AE=100/0
3	Circle, $Ø_{eff}$ = 0.938 m	3.8 (14,050)	FE/AE=100/1
4	Circle, $Ø_{eff}$ = 0.938 m, density of polythene in the core is 10.6kg/m^3	3.2 (11,920)	FE/AE=100/1
5	Square, 1x1 m	2.27 (12,330)	FE/AE=100/0
6	Square, 1x1 m	2.91 (12,790)	FE/GE=4/1

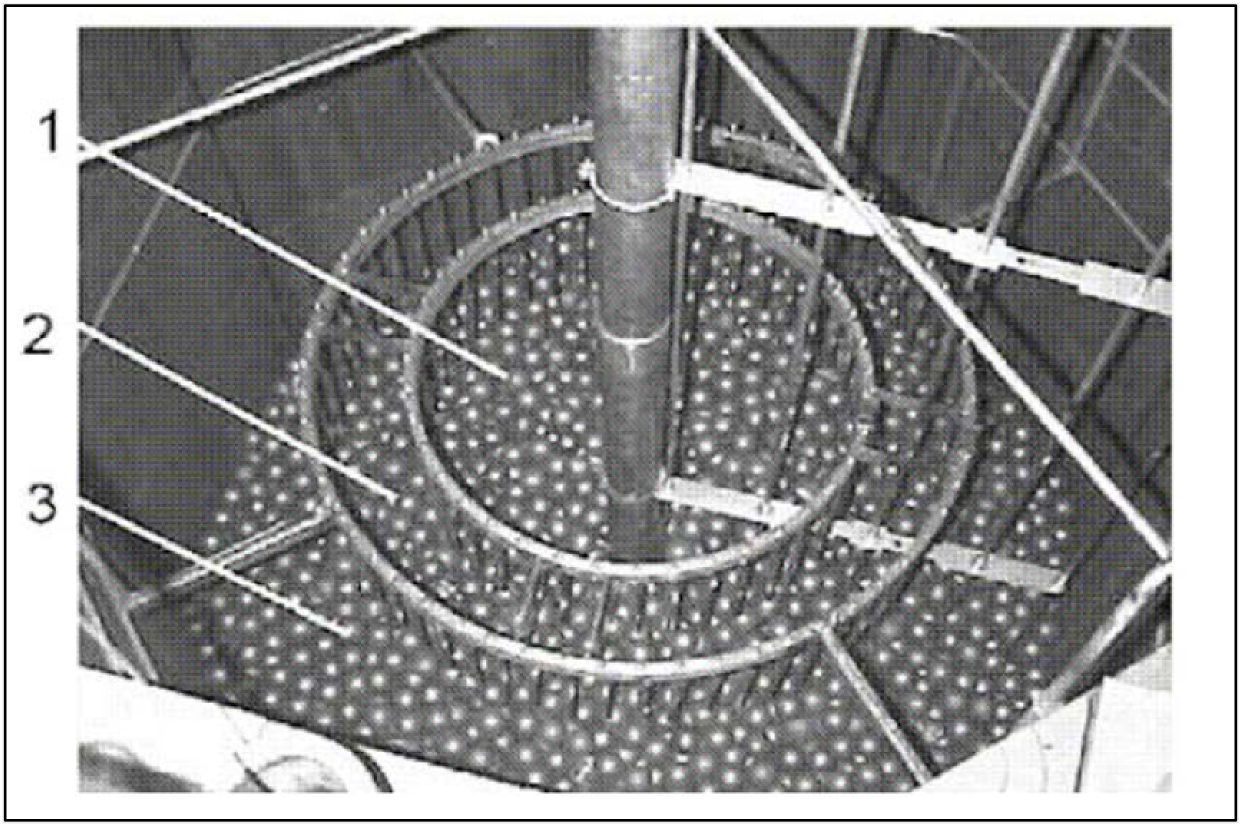

Figure 18: The ASTRA Critical Assembly

The ASTRA Critical Assembly showing the PBMR dynamic central column configuration with the 3-zone core of 1) inner reflector, 2) mixing zone and 3) the outer fuel zone.

5.1.1.3 HTR-PROTEUS

The HTR-PROTEUS facility is a zero-power test reactor operated by the Paul Scherrer Institute between 1992 to 1996. The main intent of this facility was to characterize the reactor physics of Low Enriched Uranium (LEU) in a graphite moderated pebble bed core.

The vertical cross-section of the test vessel is schematically shown in Figure 19. The facility consists of a dodecagon shaped core with the overall dimensions shown in Figure 19. A top view of the facility is shown in Figure 20.

The core is filled with 3 types of pebbles: moderator pebbles (no fuel), fuel pebbles (containing LEU), and absorber pebbles. Over the course of the HTR-PROTEUS facility operation, 10 different core arrangements were examined. The core arrangements utilize different: packing arrangements (hexagonal close-packed, Random packing or Columnar point-on-point packing), ratios of moderator to fuel pebbles, total number of pebbles, and number of polyethylene rods in the core.

The facility is equipped with 4 shutdown rods (boron) and 4 control rods (typically stainless steel but is test dependent). To simulate water ingress, without introducing water into the core, polyethylene rods of various shapes and sizes were inserted into the core. The reactor core is surrounded by reflectors on all sides and the top reflector is removable.

The HTR-PROTEUS data that is publicly available includes the following measurements for various core configurations.

- Critical loading (i.e., loading required for criticality)
- Shutdown and control rod worth (individual and for banks at varying insertion levels)
- Reflector worth
- Ratio of effective delayed neutron fraction to generation time
- $k\mathrm{eff}$ (for water ingress impact assessment)

While the HTR-PROTEUS has 10 unique core configurations, the following configurations will be used in the validation exercises as they allow for validation of water ingress and seismic impacts (i.e., higher pebble packing fractions simulating the effects of pebble compaction):

- Cores 1, 1A, 2, and 3 –

  Cores 1, 1A, 2, and 3 utilize a hexagonal close-packed (HCP) lattice configuration for the pebbles in the core. This HCP lattice configuration yields a theoretical pebble packing fraction of 0.7405, which is significantly denser than the 0.61 packing fraction typically assumed for pebble bed configurations.
- Core 4

  This core includes two cases. The first case includes a core obtained by random pebble loading using a separate fuel and moderator pebble delivery tube. For the second case, the core was obtained by random pebble loading using a single pebble delivery tube.
- Core 5

  This core utilizes a columnar point-on-point packing with a fuel to moderator pebble ratio of 2:1. This configuration does not contain any polyethylene rods and is representative of a scenario with no water ingress.
- Core 7

  This core is like Core 5, except that full length polyethylene rods have been inserted into the core to simulate water ingress.
- Core 8

  This core is like Core 5, except that short polyethylene rods have been inserted into the core to simulate water ingress in the lower portion of the core.

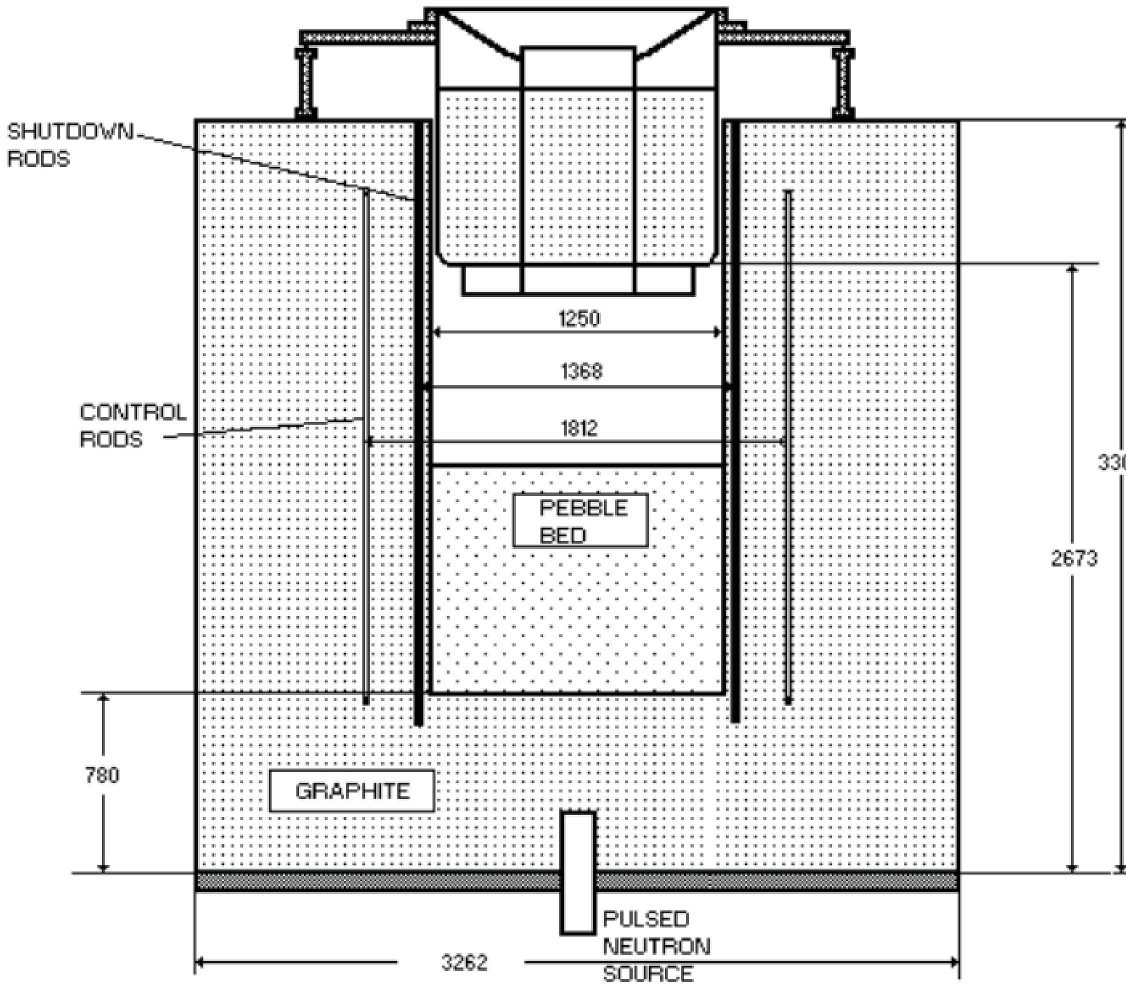

Figure 19: Schematic Side View of HTR-PROTEUS Facility (dimensions in mm)

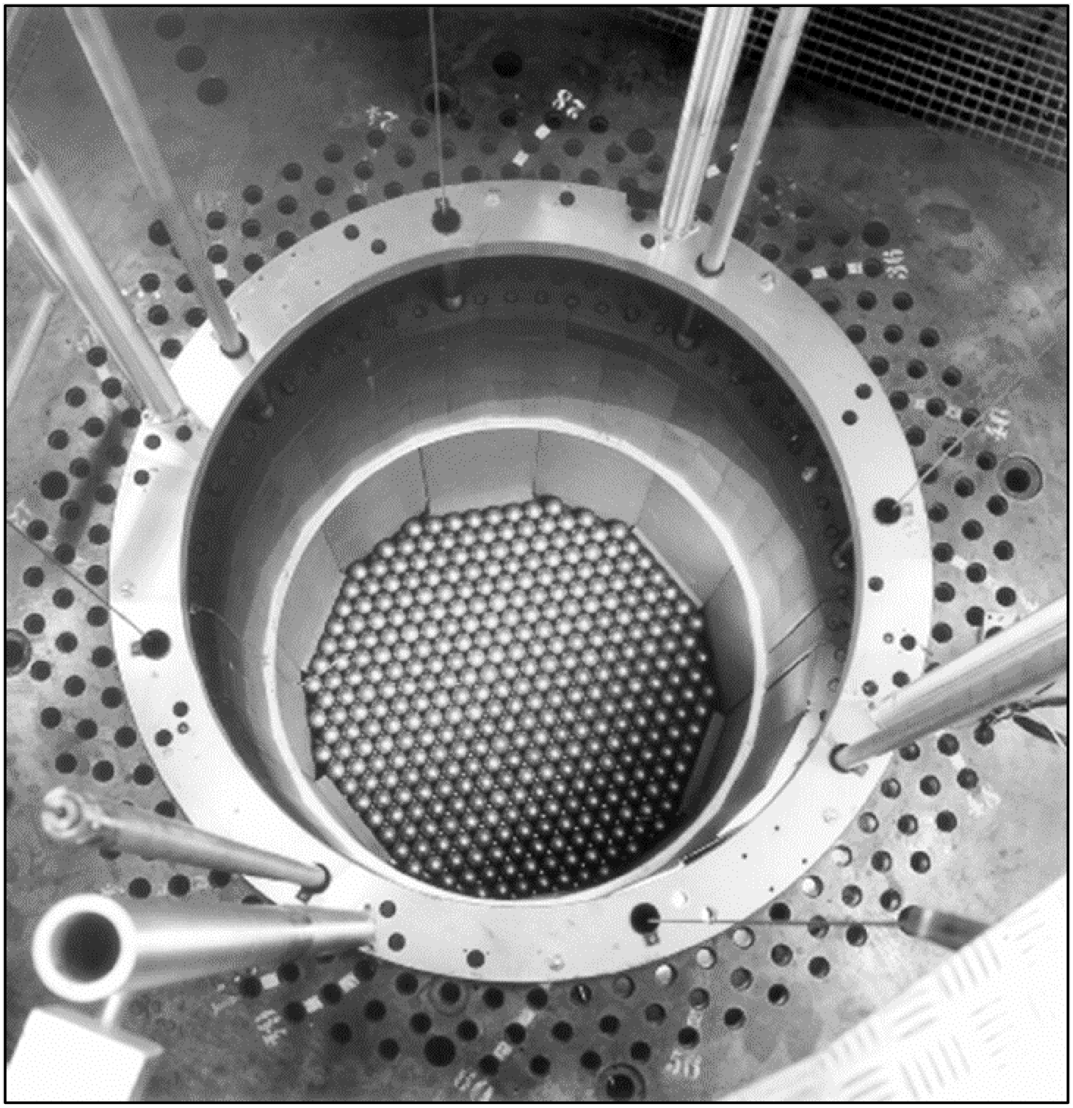

Figure 20: Top View of HTR-PROTEUS Facility

5.1.2 VSOP Validation Plan

VSOP [4] has been used for more than 30 years in the nuclear industry around the world. X-energy intends to qualify the code through comparison to experimental results as well as to code-to-code benchmarks.

5.1.2.1 VSOP Validation Against Experimental Results

X-energy intends to compare and validate VSOP [4] against the following benchmark experiments [8].

Table 9: VSOP Validation Against Experimental Results

[[

]] P

5.1.2.2 VSOP Code-to-Code Benchmarks

In addition to the validation against experimental benchmarks, VSOP [4] will also be validated against higher level codes. The following Table 10 provides the VSOP [4] benchmarks that will be performed against other higher-level codes:

Table 10: VSOP Code-to-Code Benchmarks

[[

]] P

5.2 STAR-CCM+

5.2.1 STAR-CCM+ DEM Validation General Considerations

X-energy uses the STAR-CCM+ [5], a Discrete Element Method (DEM) computational tool, to model core pebble flow characteristics in the Xe-100 core, as discussed in Section 3.3.1. The key figure of merit will be pebble residence time, in the form of a non-dimensional retention time ratio. The retention time ratio is the ratio of pebbles' in-core time through the centerline vs. at the wall. Validation of the STAR-CCM+ [5] DEM calculations for this application leverages comparisons with experimental data.

Data from several pebble flow experiments are available for validation of the DEM models developed to predict pebble behavior in the Xe-100 core. These available experiments are discussed in STAR-CCM+'s V&V plan [9], but the following will be considered for the validation basis:

1. Experiments by A. D. Bedenig at the Nuclear Research Facility in Jülich, Germany [13].
2. Multiple works by Xhonneux et al. that evaluated data from a German experiment “ANABEK” [14].

These experiments are discussed in Section 5.2.2 below.

5.2.2 STAR-CCM+ DEM Validation Data

1. D. Bedenig, a physical experiment at the Nuclear Research Facility in Jülich, Germany [13].

To estimate pebble flow behavior and trajectories in the 300 MWe THTR prototype reactor, Bedenig executed several flow experiments with pebbles of graphite, steel, glass, and clay. These experiments included several variations of bed dimensional ratios from which characteristic functions were derived to describe the flow. Friction coefficients were measured for each pebble material. shows a sample of the glass pebble experiment on the left, and the corresponding experimental and calculated results on the right.

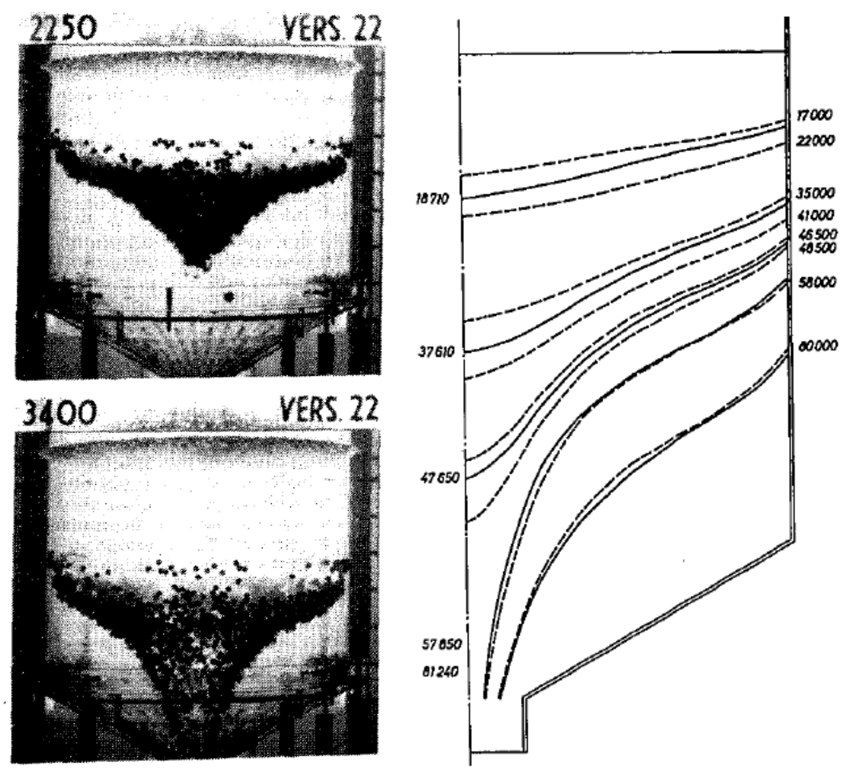

Figure 21: Experimental (left) and Calculated (right) Results as Presented by A. Bedenig

This experiment by D. Bedenig is well suited to be included when validating DEM calculations developed for the Xe-100 because (1) it included a large parametric scope with a wide variety of bed dimensional ratios and (2) the results formed a basis for the ANABEK experiment.

2. Xhonneux et al., pebble flow research which used ANABEK as its validation basis [14].

The Research Center (Forschungszentrum) in Jülich, Germany, has a rich history of testing gas-cooled high-temperature reactors. As such, this center has developed, validated, and optimized a variety of computer codes to simulate the different safety and operational aspects of HTGRs. Efforts were undertaken to integrate these various codes into one consistent package. As part of that effort, Xhonneux et al. [14] developed a code called Software for Handling Universal Fuel Elements (SHUFLE). SHUFLE was aimed at closing the gap between pebble flow predicting models that were either too coarse, and did not take localized effects into account, or too fine which were computationally intensive.

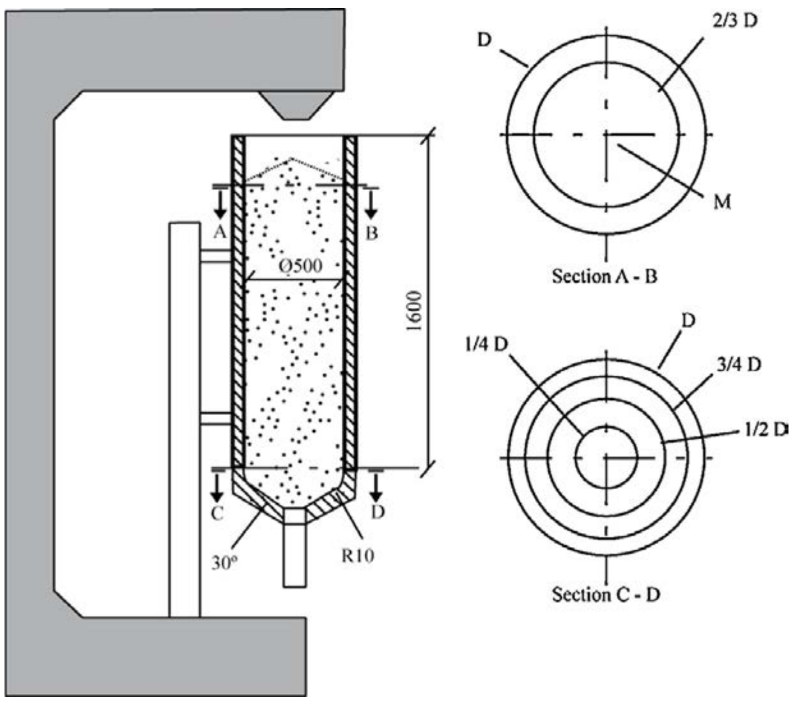

Figure 22: ANABEK Pebble Bed Flow Experiment Schematic

Xhonneux et al. [14] continued to validate SHUFLE against the ANABEK (ANAlysis of BElastungen) experiment. ANABEK was a 1/6th scale of the HTR-Module, which was a 200 MWth HTGR designed and licensed in Germany. The scaled experiment, ANABEK, facilitated understanding of the pebble flow in the full-scale HTR-Module and compared against results from D. Bedenig's experiments [13].

Even though the ANABEK experiment was scaled and manufactured from Aluminum, significant care was taken to stay true to the geometry inside the HTR-Module's core. Inter-sphere and sphere-wall friction coefficients were determined throughout the ANABEK experiments, to account for the impacts of scaling and material changes. This core contained 360,000 polyacetate spheres, scaled down to diameters of 10 mm. The ANABEK experiment is depicted schematically in Figure 22.

Importantly, the HTR-Module, and by extension the ANABEK experiment, had similar core dimensional ratios as the Xe-100. These dimensional ratios refer to (1) the ratio of the core height to the diameter, (2) the ratio of the core diameter to the pebble diameter, (3) the ratio of the defuel chute diameter to the pebble diameter, and (4) the outlet funnel's conical angle to the horizontal plane. Thus, the core's geometric parameters which impact pebble flow are similar between the Xe-100, the HTR-Module, and the ANABEK experiment, regardless of scale.

Results of the ANABEK experiment are primarily depicted as the extracted percentage of a defined (marked) layer of pebbles, which was initially set at the top of the bed, as a function of the percentage of pebbles cycled. In other words, as the pebbles are cycled and the defined (marked) pebbles exit at the bottom, their exit time is recorded in relation to the total number of pebbles cycled. The retention time ratio is then calculated from the results. Xhonneux et al. [14] compared these results when successfully validating SHUFLE against the ANABEK experiment and a similar approach will be followed when validating the DEM calculations developed for the Xe-100.

5.2.3 STAR-CCM+ Validation Plan

Initial evaluation of these experiments, according to Section 6.2.1, shows that the works by Xhonneux et al. [14], of the German ANABEK experiment, will be suitable for validation purposes. Thus, this experiment will be simulated with STAR-CCM+ [5] and compared with the experimental results to validate the computational method. Modeled residence times will be evaluated according to the following Figures of Merit (FOM):

- Residence time ratio: a non-dimensional measure of pebble residence time normalized against the recirculation frequency.
- Retention time ratio: a ratio of pebbles' in-core time through the centerline vs. at the wall.

Results for these ratios within 10% of the experimental values will be deemed acceptable for this validation activity.

5.3 Validation Reports

Each new validation exercise will be documented in a standalone report. A final summary report will also be created to summarize the existing and new validation that supports VSOP [4] and STAR-CCM+ [5].

6. Verification Plan and Validation Method

6.1 Verification Plan

Verification shall be done on each validation exercise and on the reports that are generated to document the validation exercises. Verification of the validation exercises shall include checks of the following, where applicable:

a. Evidence that the validation exercise followed the validation plan.
b. Evidence that the code version applied in the validation exercise is consistent with that applied in the Xe-100 safety analysis.
c. Confirmation that the models applied in the validation exercise correctly represent the experimental, or analytical configurations. This includes checking that the geometry, material properties, and boundary conditions have been correctly incorporated into the model.
d. Confirmation that the correlations applied in the validation exercise are consistent with the correlations and models applied in the Xe-100 safety analysis.
e. Confirmation that the analysis performed to determine the discretization required for grid independence is correct and rational and that grid independence has been achieved.
f. Confirmation that the simulations have been executed without error and that the results are rational.
g. Confirmation that the benchmark data is suitably qualified for use in the validation exercise.
h. Confirmation that the calculation of the bias and variation in the bias, and the calculation of the normalized point difference is correct.

6.2 Validation Method

For each validation exercise, the steps described below will be followed in accordance with X-energy Quality Assurance Program (QAP), which is discussed in Section 7.

6.2.1 Qualification of Data

The following will be documented to support the use of the experimental data in the validation exercise:

a. Confirmation that the experimental facility is adequately described.
b. Disposition differences between experimental and plant design conditions.
c. Disposition differences between the range of conditions covered in the experiments and those expected in the plant.
d. Confirmation that the tests and the measured data have been studied in sufficient detail and that the overall behavior and responses of the experiment are well understood.
e. Determine if measurement uncertainties are documented.
f. Assess if the experiments have been conducted with sufficient accuracy and precision.
g. Assess the availability of the data in electronic form.

h. The data will also be reviewed for consistency and correctness (i.e., it should not appear to be erroneous).

6.2.2 Preparation of Models

Models will be developed for each of the validation exercises. The models will be documented, with references supporting the geometric, material property, and boundary conditions used in the construction of the model.

6.2.3 Code Accuracy Calculations

The predictions will be compared to the test data using the convention typically applied in the nuclear industry. The convention is to calculate the code bias and variation in the bias. The code bias calculation is the average value of the residuals as shown below:

$$\boldsymbol{bias = R_{average} = \frac{1}{N}\sum_{t=t_1}^{t=t_N} R(t_i)} \quad (42)$$

Where:

- $R(t_i) = M_i - C_i$ is the residual at a specific point in time or space,
- M_i is the measured value,
- C_i is the predicted value,
- N is the number of the point in time or space at which the code and measurement are compared, and
- t_i represents a specific point in time or space.

The variation in the bias calculation is the standard deviation of the residuals as shown below:

$$\boldsymbol{variation\ in\ bias = \sqrt{\frac{\sum_{t=t_1}^{t=t_N}\left(R(t_i) - R_{average}\right)^2}{N-1}}} \quad (43)$$

6.2.4 Assessment of the Model Predictions

The model predictions will be assessed for rationality and compared against the acceptance criteria of an arbitrary 10% normalized point difference. However, acceptance criteria specific to each validation exercise may be defined if appropriate.

7. Quality Assurance

X-energy developed and implemented a Quality Assurance Program (QAP) which implements X-energy's Topical Report XEQAPD-NP, "Quality Assurance Program Description," Revision 3 submitted to the NRC in August of 2020 [26]. The X-energy QAPD is based on the applicable portions of both Appendix B, "Quality Assurance Criteria for Nuclear Power Plants and Fuel Reprocessing Plants," to, Title 10 of the Code of Federal Regulations Part 50, "Domestic Licensing of Production and Utilization Facilities," (10 CFR 50) and American Society of Mechanical Engineers (ASME) NQA-1-2015, "Quality Assurance Program Requirements for Nuclear Facilities," as endorsed by NRC Regulatory Guide (RG) 1.28, "Quality Assurance Program Criteria (Design and Construction)," Revision 5. The NRC reviewed this report and determined that X-energy XEQAPD Revision 3 satisfies the quality assurance requirements of Appendix B to 10 CFR 50 (ADAMS Accession No. ML20233A910). The activities described in this LTR are subject to, and conducted in accordance with, the provisions of the approved X-energy QAPD.

8. Conclusions and Limitations

8.1 Conclusions

This report describes the Xe-100 reactor, the physical characteristics of the core, the modeling of the reactor, and the applicability of the codes and methods used in the analysis. The codes and methods described herein can be used by prospective applicants to support their licensing basis for construction permits or operating licenses.

The codes and methods described in this report can be used for core design, fuel management studies, and calculating input to the safety analyses. The principal codes employed are VSOP and STAR-CCM+. VSOP is used for the neutronics and thermodynamic analysis and STAR-CCM+ is used to simulate the movement of fuel pebbles through the reactor, providing input to VSOP.

Code validation for VSOP is performed by comparing the code results to experimental data from other HTGR facilities. In addition, benchmark calculations compare VSOP results to those of MCNP for parameters including reactivity coefficients, effective neutron multiplication factors, and control rod worths. STAR-CCM+ is validated by comparison of pebble flow through physical models. A plan has been developed to verify these validation activities. When the validation and verification of the codes as described in this report are complete, X-energy will submit the results to the NRC, either as a revision to this topical report or as a stand-alone document, for approval for purposes of supporting an operating license. The submittal will include specific uncertainty values and will be completed before the submittal of an FSAR.

8.2 Limitations

X-energy is requesting NRC review and approval of the methodology and computer codes described in Sections 3, 4, 5 and 6 of this LTR for use in Xe-100 license applications as an appropriate means to perform steady-state and normal operations physics analysis and to provide appropriate inputs to support the Xe-100 safety analyses, subject to the following limitation:

> Until validation and verification of the VSOP and STAR-CCM+ codes as described in this report are complete and have been approved by the NRC, the codes and methodology described herein cannot be used to support a final safety analysis report.

9. Cross References and References

9.1 Cross References and References

	Document Title Cross References: X-energy documents that <u>may</u> impact the content of this document. References: X-energy or other documents that <u>will not</u> impact the content of this document	Document No.	Rev./ Date of Issuance	Cross Reference/ Reference
[1]	Topical Report EPRI-AR-1(NP)-A, Uranium Oxycarbide (UCO) Tristructural Isotropic (TRISO)-Coated Particle Fuel Performance	EPRI_AR-1(NP)-A	November 2020	Reference
[2]	X-energy Licensing Topical Report, "Xe-100 Principal Design Criteria Licensing Topical Report"	004799	Rev. 3 February 2024	Reference
[3]	X-energy Report, "Xe-100 Physical Configuration Summary Report"	000780	Rev. 2 December 2020	Reference
[4]	V.S.O.P. (99/05) Computer Code System for Reactor Physics and Fuel Cycle Simulation	VSOP (99/05) IAEA RN:37024454	October 2005	Reference
[5]	Siemens Simcenter STAR-CCM+ Computer Code Version 2206	---	2022	Reference
[6]	X-energy Licensing Topical Report, " TRISO-X Pebble Fuel Qualification Methodology"	000633	Rev. 3 July 2022	Reference
[7]	World Nuclear News Article, https://www.world-nuclear-news.org/Articles/Chinese-HTR-PM-Demo-begins-commercial-operation	--	December 2023	Reference
[8]	X-energy Report, "X-energy Physics Code Suite Validation Plan"	002101	Rev. 3 November 2023	Reference
[9]	X-energy Report, "Simcenter START-CCM+ V&V Plan"	006617	Rev. 3	Reference
[10]	X-energy Design Information Transmittal, "Preliminary Scoping 200 MWth Steady-State Equilibrium Core Design Analysis"	009331	Rev. 1 December 2023	Reference
[11]	Plant Engineering: Guideline for the Acceptance of Commercial-Grade Design and Analysis Computer Programs Used in Nuclear Safety-Related Applications, Rev. 1	TR -1022543	December 2013	Reference
[12]	E Teuchert, HJ Rütten and KA Haas: Rechnerische Darstellung des HTR-MODUL-Reaktors, FZJ report, Jül-2618	--	May 1992	Reference
[13]	D. Bedenig, "Ein theoretisches model zur beschreibung des kugelhaufen-fliessverhaltens im core eines kugelhaufen-reaktors A theoretical model for the description of the spherical bed flow behavior in the core of a globular bed	doi.org/10.1016/0029-5493(67)90091-X	1967	Reference

	Document Title Cross References: X-energy documents that may impact the content of this document. References: X-energy or other documents that will not impact the content of this document	Document No.	Rev./ Date of Issuance	Cross Reference/ Reference
	reactor],” Nuclear Engineering and Design, Vol. 6, p. 479-488, 1967.			
[14]	A. Xhonneux, S. Kasselmann, H. J. Rütten, K. Becker, and H. F. Allelein, “Progress on the development of a new fuel management code tosimulate the movement of pebble and block type fuel elementsin a very high temperature reactor core,” Nuclear Engineering and Design, Vol. 271, p. 370-378, 2014.	doi.org/10.1016/j.nucengdes.2013.12.004	2014	Reference
[15]	Friederike Bostelmann, Erik D. Walker, Steve E. Skutnik, Germina Ilas, and William A. Wieselquist, “Relevant Advanced Reactor Benchmarks for Nuclear Data Assessment”	ORNL/SPR-2020/1665	September 2020	Reference
[16]	W.K. Terry, J.K. Jewell, J. Blair Briggs, T.A. Taiwo, W.S. Park, and H.S. Khalil, “Preliminary Assessment of Existing Experimental Data for Validation of Reactor Physics Codes and Data for NGNP Design and Analysis”	ANL-05/05	2004	Reference
[17]	Korea Atomic Energy Research Institute, “Status of Experimental Data for the VHTR Core Design”, KAERI	KAERI/AR-702/2004	2004	Reference
[18]	International Atomic Energy Agency, “Evaluation of High Temperature Gas Cooled Reactor Performance: Benchmark Analysis Related to the PBMR-400, PBMM, GT-MHR, HTR-10 and the ASTRA Critical Facility”, IAEA	IAEA-TECDOC-1694	2013	Reference
[19]	“Experimental Facilities for Gas-cooled Reactor Safety Studies”, NEA Doc. No.	NEA/CSNI/R (2009)8	2009	Reference
[20]	X-energy Procedure, Commercial Grade Dedication of Items and Services Procedure	QAP 7.5	Rev. 1 April 2022	Reference
[21]	"Berechnung der Nachzerfallsleistung der Kernbrennstoffe von Hochtemperaturreaktoren mit kugelförmigen Brennelementen" DIN 25485 (1990), Deutsches Institut für Normung eV, Postfach 1107, D-1000, Berlin 30	DIN 25485	1990	Reference
[22]	U.S. NRC Policy Statement on the Regulation of Advanced Reactors	73 FR 60612	2008	Reference
[23]	Quality Assurance Requirements for Nuclear Facility Applications	ASME NQA-1	2015	Reference
[24]	Plant Engineering: Guideline for the Acceptance of Commercial-Grade Design and Analysis Computer Programs Used in Nuclear Safety-Related Applications	TR -1022543	Rev. 1 December 2013	Reference
[25]	NRC Regulatory Guide 1.231, Acceptance of Commercial-Grade Design and Analysis Computer Programs Used in Safety-related Applications for Nuclear Power Plants	RG 1.231	January 2017	Reference

Document Title Cross References: X-energy documents that <u>may</u> impact the content of this document. References: X-energy or other documents that <u>will not</u> impact the content of this document		Document No.	Rev./ Date of Issuance	Cross Reference/ Reference
[26]	X-energy Licensing Topical Report "Quality Assurance Program Description"	XEQAPD 1.0 ADAMS Accession No. ML 20220A413	Rev. 3	Reference
[27]	X-energy Report, "Software Procedure"	QAP 3.6	Rev. 3	Reference
[28]	Risk-Informed Performance-Based Technology Inclusive Guidance for Non-Light Water Reactor Licensing Basis Development	NEI 18-04	1	Reference
[29]	Guidance for a Technology-Inclusive, Risk-Informed, and Performance-Based Methodology to Inform the Licensing Basis and Content of Applications for Licenses, Certifications, and Approvals for Non-Light Water Reactors	1.233	June 2020	Reference
[30]	Xe-100 Licensing Topical Report, "Transient and Safety Analysis Methodologies"	007834	Rev. 1	Reference
[31]	Xe-100 Licensing Topical Report, "Mechanistic Source Term Approach"	000632	2	Reference
[32]	Fen, V., Lebedev, M., Sarytchev, V., Scherer, W., "Modeling of Neutron Absorbers in High Temperature Reactors by Combined Transport-Diffusion Methods"	KFA-Jülich Report, Jül-2573	1992	Reference
[33]	Reitsma, F., Naidoo, D., "Evaluating the control rod modeling approach used in the South African PBMR: comparison of VSOP calculations with ASTRA experiments"	Nuclear Engineering and Design	2003 (222 147-159)	Reference
[34]	Xe-100 Licensing Topical Report, "GOTHIC and Flownex Analysis Codes Qualification"	1	2024	Reference
[35]	Xe-100 200MWth Preliminary Steady-State Core Design Report	5	2022	Reference